C.P. No. 103
(14,448)
A.R.C. Technical Report

MINISTRY OF SUPPLY

AERONAUTICAL RESEARCH COUNCIL

CURRENT PAPERS

Some Effects of Reynolds Number on a Cambered Wing at High Subsonic Mach Numbers

By

H. E. Gamble, B.Sc.

LONDON: HER MAJESTY'S STATIONERY OFFICE

1952

Price 5s. 0d. net

C.P. No. 103

Report No. Aero 2423

May 1951

ROYAL AIRCRAFT ESTABLISHMENT

Some effects of Reynolds number on a cambered wing at high subsonic Mach numbers

by

H.E. Gamble, B.Sc.

SUMMARY

An untapered, sweptback wing of aspect ratio 4, sweepback 25° and section 12% thick (R.A.E. 104 with 1% camber, a = 0.6) was tested in the R.A.E. High Speed Tunnel. The pressure distribution was measured at the mid-semispan section at various Mach numbers up to 0.88 at Reynolds numbers of 0.8, 1.8 and 3.5×10^6.

There are considerable differences in the shapes of the pressure distributions at the three Reynolds numbers, although the boundary layer was laminar back to about 70% of the chord in all cases. At the highest Reynolds number, the suctions on the upper surface at high Mach numbers increase from the leading edge of the wing right up to about 50% or 60% of the chord, while at the lowest Reynolds number they remain almost constant from about 30% to about 60% of the chord. This flat-topped pressure distribution, which is associated with a λ-type shock wave, results in lower lift coefficients and higher pitching moment coefficients than those obtained at higher Reynolds number.

Brief experiments, with transition provoked near the leading edge, indicate that the shape of the pressure distribution at $R = 0.8 \times 10^6$ is then something similar to that obtained at $R = 3.5 \times 10^6$ with transition free and at about 65% chord. It appears, however, that inducing early transition artificially at higher Reynolds numbers can seriously alter the pressure distribution at high speed by causing a forward movement of the shock wave and a separation aft of it.

LIST OF CONTENTS

LIST OF TABLES

LIST OF ILLUSTRATIONS

1 Introduction

Some time ago various tunnel tests giving the overall forces on models of a modern aircraft indicated that there were large Reynolds number effects up to 3 or 4 × 10^6 at high speeds. It was, therefore, decided to pressure plot a wing of similar section and sweepback in the R.A.E. High Speed Tunnel to investigate the associated changes in pressure distribution and also to shed some further light on the general problem.

The wing section chosen for the tests was R.A.E.104, 12% thick with 1% camber (a = 0.6). (Table I). The wing was also used to investigate some points of testing technique in the Tunnel.

2 Details of Model

The tests were made on a constant chord teak model supported on the floor of the R.A.E. High Speed Tunnel. The model was chosen to be as large as possible, consistent with a reasonable value of the choking Mach number, so that (a) end effects would be negligible at the test section, and (b) the maximum Reynolds number would be as high as possible. The chord was chosen to be 2 feet, the semi-span (from root to tip) was 4 feet, and the wing was sweptback 25°.

Forty four pressure plotting holes were inserted at the mid semi-span of the wing at 5% intervals along the chord and also at 0.75 and 2.5% of the chord on both surfaces.

The wing was finished with black "phenoroc" to enable the chemical sublimation method[1] to be used to indicate the position of boundary layer transition from laminar to turbulent flow. In this method the wing is sprayed with a 4½% solution of acenapthene in light petroleum ether and acetone. This leaves a thin white film over the surface of the wing. The film evaporates rapidly in regions where the boundary layer is turbulent and much more slowly in regions of laminar flow, so that after running the tunnel for 10 to 20 minutes at the required speed and incidence, the white film is still present in the laminar flow regions, but the wing is quite clean (and black) in regions of turbulent flow.

3 Range of Tests

The wing was tested during April 1950, some check tests being made in October 1950.

The main tests consisted of pressure distribution measurements at nine Mach numbers up to 0.88 at Reynolds numbers of 0.8 × 10^6, 1.8 × 10^6 and 3.5 × 10^6 at incidences of approximately -1°, 0°, 1.5° and 3.0°.

The position of boundary layer transition was found to be between 65% and 70% of the chord in these tests. Further tests were, therefore, made with the transition position brought forward by artificial means. Threads were attached to both surfaces of the wing along the span. When a successful choice of thread size and position was found at M = 0.82 and α = 0°, the pressure distribution was measured over the same range of Mach numbers and Reynolds numbers as with transition free but only at incidences of 0° and 3°.

An attempt was also made to provoke forward transition by placing a 16 gauge wire in the chord plane about half a chord length ahead of the leading edge of the wing. At $R = 0.8 \times 10^6$, $M = 0.82$ and $\alpha = 0^\circ$ transition appeared to have been brought forward to about 30% of the chord, so pressure distributions were measured at the same Reynolds numbers and Mach numbers as before, but at $\alpha = 0^\circ$ only.

4 Presentation of Results

Blockage corrections were applied to Mach number and C_p according to the method of Ref.2. At the highest Mach number of the tests the blockage correction to the uncorrected Mach number was 0.027 and the correction to C_p was 0.08 for a C_p of -0.8.

No correction was applied to incidence for the effect of tunnel constraint. This correction, which may be about 0.3° at the highest lift coefficients of the test would not affect the comparisons made in the report, although it would slightly lower the values of the slope of the lift curve.

Since the tests were made primarily to find the effect of Reynolds number on the transition-free pressure distribution of the wing, all the results relating to this are presented first (Figs. 2 to 14). In the later figures (15 to 20) and discussion the results of the transition-fixed tests are given.

Pressure distributions are shown only for a few typical Mach numbers and Reynolds numbers, Figs. 2 to 4 and 15 to 17.

The lift and pitching moment coefficients were found at $R = 3.5 \times 10^6$ by integrating with respect to x/c the difference in pressure, ΔC_p, between the upper and lower surfaces of the aerofoil. The amounts by which these C_L and C_m values differed from those at $R = 1.8 \times 10^6$ 0.8×10^6 were then found by integrating with respect to x/c the difference between the values of ΔC_p at each pair of pressure holes at $R = 3.5 \times 10^6$ and the corresponding values of ΔC_p at $R = 1.8 \times 10^6$ and 0.8×10^6. Thus the differences in C_L and C_m due to Reynolds number were obtained more accurately than if each case had been integrated completely independently. (This work was all done on the R.A.E. Differential Analyser, mainly because it was less tiring to use than the Amsler Integrator.)

Later, C_L and C_m were estimated for the transition fixed cases by a simple numerical integration, which was reasonably accurate in view of the close spacing of the pressure holes.

Form drag coefficient was found by integrating C_p against y/c in the transition free cases, but owing to the labour involved it was evaluated for only one case with transition fixed, viz: $R = 3.5 \times 10^6$ and $\alpha = 0^\circ$.

The integrated values of C_L, C_D and C_m and their derived functions are shown in Figs. 7 to 14 and 19 and 20.

The results of all the tests made with the transition indicator present are given in Table II. Some photographs illustrating special points are given at the end of the report (Figs. 21 and 22).

5 Results

5.1 Transition free (at 65 to 70% chord)

5.11 Low speed results. (Fig. 2)

At Mach numbers of 0.5 and 0.7 the pressure distribution curves agree closely at the three Reynolds numbers of test except between 65% and 80% of the chord. It is probable that the observed increase in suction here at low Reynolds number is caused by a slight boundary layer separation and subsequent reattachment of the flow. This effect becomes more noticeable with increase in Mach number until it is masked by the shock wave.

5.12 High speed results (above M = 0.8). (Figs. 3 to 14)

At higher Mach numbers when there is a shock wave on the wing large changes in pressure distribution become apparent on both surfaces. At the highest Reynolds number, 3.5×10^6, the suction increases steadily from the leading edge to about 60% of the chord and then there is a fairly abrupt increase in pressure through the shock wave. At the lowest Reynolds number, 0.8×10^6, the suction remains almost constant from about 30 or 40% of the chord to about 60%, giving a very flat-topped pressure distribution; also as full a pressure recovery is not achieved at the trailing edge. The shape of the pressure distribution at low Reynolds number is associated with a thick boundary layer, the flow being laminar at all the Reynolds numbers of test.

Ackeret[3] found similar changes with Reynolds number in the pressure distribution on a curved plate and associated the flat distribution at low Reynolds number with a "λ" shock. His work would suggest that the first slight rise in pressure occurred at the first limb of the λ shock wave and the main rise in pressure at the rear limb. Ackeret found in his tests that the flow had separated between the limbs, reattaching itself as a turbulent layer at the main limb. It was therefore suspected that the flow was separated on the wing in the present tests at $R = 0.8 \times 10^6$ and some confirmation of this was obtained by using the chemical transition indicator described in section 2 and also by using tufts. Figs. 6 and 21 show how the transition indicator evaporated from the wing surface at M = 0.82, $R = 0.8 \times 10^6$ and $\alpha = 0^\circ$. The development during the first 40 minutes was normal, but the front edge of the indicator usually continues to retreat rapidly backwards until all the indicator has disappeared. In this case there was a marked tendency during the last 15 minutes of the tests for the indicator to remain in the region where it was expected that the flow was separated. Some further evidence was obtained from nylon tufts which were put on the wing between 50% and 70% of the chord. Unfortunately the tufts seemed to cause a slight increase in $-C_p$ of about 0.08 between 40% and 65% chord,

although they did not bring the transition forward by more than 5% of the chord. In Fig. 22 it can be seen from the random arrangement of the tufts that the flow is separated at least aft of 60% chord at $R = 0.8 \times 10^6$, $M = 0.82$, $\alpha = 0^\circ$. A test made at $R = 3.5 \times 10^6$ and at the same Mach number and incidence showed the tufts to be neatly aligned along the wing chord.

The only other large difference in the pressure distributions is on the lower surface where the separation which occurred at low speed at $R = 0.8 \times 10^6$ between 60% and 80% of the chord became more and more marked as the Mach number increased.

The effect of Reynolds number on the values of C_L, C_D and C_m obtained by integration of the pressure distribution curves is quite large. As the Reynolds number is increased the loss of C_L with increasing Mach number occurs later and becomes less severe (Fig. 7) and the value of C_m becomes more nose down (Fig. 12). The drag rise is also delayed by about 0.013 in Mach number as the Reynolds number is increased from 0.8 to 1.8×10^6, but there is not much further change between 1.8 and 3.5×10^6 (Fig. 10). There are large changes in the lift curve slope (Fig. 13) and in the position of the aerodynamic centre (Fig. 14).

The flattening of the upper surface pressure distribution as the Reynolds number is decreased accounts for most of the loss in lift coefficient and increase in nose up pitching moment coefficient between $R = 3.5$ and 1.8×10^6 and about half of these effects between $R = 1.8 \times 10^6$ and 0.8×10^6. The remaining decrease in C_L and increase in C_m at the low Reynolds number probably comes from the separated region between 60% and 80% chord on the lower surface. This is also mainly responsible for the increase in drag coefficient between $R = 1.8 \times 10^6$ and 0.8×10^6. At low incidences some of the increase in drag is caused by the increased trailing edge suctions at low Reynolds numbers, but at higher incidences the trailing edge suctions are practically the same at all three Reynolds numbers.

5.2 Comparison with N.P.L. tests on R.A.E. 104 section, 10% thick

Two aerofoils of 2 inches and 5 inches chord and section R.A.E. 104, 10% thick were tested in the N.P.L. 20" × 8" High Speed Tunnel, and the tests are reported in Ref.[4]. The Reynolds numbers obtained at a Mach number of about 0.8 are 0.7×10^6 and 1.8×10^6 and hence are comparable with the two lower Reynolds numbers in the R.A.E. tests.

In general the N.P.L. results agree very closely in character with the results of the present tests. At about 0.7 of the chord at low Mach numbers there is a laminar boundary layer separation, which increases as the Mach number increases. At Mach numbers above 0.8 the characteristic flat-topped pressure distribution is again apparent, particularly at the lower Reynolds number, and has been associated by schlieren photographs with a separation aft of the front limb of a λ type shock wave. As in the R.A.E. tests, the separation occurs slightly further

back along the chord at the higher Reynolds number. The measured pressure rise through the shock wave is steeper at the higher Reynolds number and at zero incidence the pressure recovery is much more complete at the trailing edge.

5.3 Transition fixed (see Table II)

The changes in pressure distribution caused by fixing the transition forward on the aerofoil are shown in Figs. 15 to 17.

In general the local separations apparent with transition free at $R = 0.8 \times 10^6$ on both the upper and lower surfaces are abolished and the pressure distribution curves follow closely the shape of the distribution at $R = 3.5 \times 10^6$. At the higher Reynolds numbers of 1.8×10^6 and 3.5×10^6, however, although the λ shock system is no longer evident and the peak suctions rise to a maximum just ahead of the main shock wave, the shock wave itself is further forward and there is a separation behind it (Fig. 18).

The effect on C_L and C_m of fixing transition at $R = 0.8 \times 10^6$ is to bring the values much closer to those obtained at $R = 3.5 \times 10^6$ with transition free (Figs. 19 and 20). On the other hand at $R = 3.5 \times 10^6$ with transition fixed the effect of the forward movement of the shock wave mentioned above, is to give C_L and C_m curves which follow more closely the transition free curves at $R = 0.8 \times 10^6$ than those at $R = 3.5 \times 10^6$.

As mentioned in section 4, C_D has been evaluated for transition fixed with threads on the wing surfaces only at $\alpha = -0.5^\circ$ and $R = 3.5 \times 10^6$. The values, which are not plotted, show an increase at all Mach numbers of about 0.003 above those at $R = 3.5 \times 10^6$ with transition free.

The results obtained with a 16 gauge wire ahead of the wing leading edge agree closely with those obtained with threads on the wing surfaces (Fig. 17). The wake behind the wire was found to be about 1.5" wide at the leading edge of the wing.

5.4 Additional tests

5.41 Fixing transition by a jet of air near the leading edge

As an alternative method of fixing transition, the effect of a small jet of air issuing from the wing near the leading edge was tried. To do this the pressure holes at 15% chord on both surfaces were connected up to valves in the observation room. Since the tunnel was at a low pressure ($\frac{1}{2}$ to $1/10$ of an atmosphere) sufficient air was sucked in when the valves were opened to start a transition wedge (Fig. 23). The centre line of the wedge was at an angle of 5° to the wing chord, and as the wedge angle was only about 5° at the low Reynolds number and high Mach

numbers, the pressure plotting holes were still in a region of laminar boundary layer flow. Opening the valves therefore had little effect on the pressure distribution, merely increasing the suctions on the upper surface slightly.

It was interesting to watch the effect of the air jet on the upper surface when the wing was tufted at $R = 0.8 \times 10^6$ at $M = 0.82$. With the valve closed the last three columns of tufts were blowing around in a random manner, but a few seconds after opening it all the tufts in the row below the pressure plotting section aligned themselves along the chord (Fig. 22).

5.42 Thread in supersonic region

A test was made with a 0.015 inch diameter thread at 37% chord to find the effect on the pressure distribution of a thread in the supersonic region. At $M = 0.82$ and $R = 0.8 \times 10^6$ transition was brought forward only to 65% chord, but the shape of the pressure distribution is nearer that obtained at $R = 3.5 \times 10^6$ with transition free. The thread seems to have no other serious effects on the wing apart from a very slight increase in pressure at the 35% hole.

At $R = 3.5 \times 10^6$, the thread causes an appreciable increase in pressure ahead of it, and at the higher Mach numbers there is a forward movement of the shock wave and a separation aft of it.

6 Summary of Results and Concluding Remarks

At the lowest Reynolds number, the boundary layer, which is laminar back to the shock wave, is thick and the shock wave is of the λ type. The first limb, noted on the pressure distribution by a small increase in pressure, is associated with the beginning of a separation of the boundary layer. In the region of separated flow the pressure is almost constant up to the main limb where there is a fairly gradual pressure recovery. On increasing the Reynolds number the position where the separation occurs moves back along the chord so that, at 3.5×10^6, the first limb has disappeared. There is then no region of constant pressure and the suction rises continuously to just ahead of the shock wave. The subsequent pressure rise is then fairly steep. Although the boundary layer is still laminar up to the shock wave this pressure distribution is probably the same as would be obtained in transition free flow with a turbulent boundary layer.

The above Reynolds number effects may be expected on most aerofoils, although they are probably not so important on thinner sections. They have been noticed on several sections, e.g. NACA 23021[5], NACA 0015[6] and, as mentioned above, on the 10% thick R.A.E. 104 section[4]. This suggests that such effects are not confined to thick cambered sections.

The effect on C_L, C_D and C_m is that the changes in these coefficients as the Mach number is increased, associated with the onset of shock waves, occur at a lower Mach number when the Reynolds number is low. Thus the Mach number at which the C_L collapses and the C_m and C_D begin to rise

decreases as the Reynolds number is decreased. This means that the no lift angle and the value of C_{m_o} both increase as the Reynolds number is decreased. Further, at low incidences, before the suction peak moves forward on the aerofoil scale effects probably increase with increasing incidence. Therefore, at low incidences, the lift curve slope decreases, and there is a forward movement of the aerodynamic centre, when the Reynolds number is lowered.

In general it may be concluded that fixing transition forward on the wing at low Reynolds numbers (say under 1×10^6) removes the main troubles caused by a thick laminar boundary layer. However, as a method of providing results similar to those which would be obtained with a turbulent boundary layer at high Reynolds number, it must be treated with some reserve. It seems that at some Reynolds numbers (say $> 10^6$), the pressure distribution so obtained does not agree, as to the position of the shock wave and the amount of separation at the trailing edge, with the distribution obtained when the boundary layer flow is laminar but is thin enough for the λ shock wave system to have disappeared.

It cannot be stated conclusively which pressure distribution is most representative of flight conditions, since it has not been shown yet whether there are still further pressure distribution changes in going from the thin laminar boundary layer flow at $R = 3.5 \times 10^6$ to naturally turbulent boundary layer flow at a higher Reynolds number.

All the above transition free effects were found in the tests on the model of a complete aircraft on which the wing in the present tests was based. In general, tests made in the R.A.E. High Speed Tunnel are at a Reynolds number of 1.5 to 2×10^6 based on the mean chord of the wing. Thus it is possible that some of the spurious effects discussed in this note may be present particularly towards the tips of tapered wings where the local Reynolds number is lower still. Every effort is made to keep the Reynolds number as high as possible and to look out for possible trouble from scale effects. As fixing transition seems to abolish the λ shock system and its associated separation and hence the main scale effect troubles at low Reynolds number, tests are often made both with transition free and with transition fixed. If there is no appreciable difference in the results it is assumed that Reynolds number effects are not important on lift or longitudinal stability below the stall.

LIST OF SYMBOLS

c — wing chord

x, y — co-ordinates of any point on pressure plotting section

ϕ — angle of sweepback of wing

α — wing incidence to air stream

M — Mach number of free stream

M_L — Local Mach number in direction normal to wing leading edge

R — Reynolds number based on wing chord

C_p — pressure coefficient

$C_{p_c}^*$ — pressure coefficient corresponding to $M_L = 1$

C_n — integrated force coefficient normal to the wing chord

$$= \int C_p \, d\left(\frac{x}{c}\right)$$

C_c — integrated force coefficient along the wing chord

$$= \int C_p \, d\left(\frac{y}{c}\right)$$

C_L — Lift coefficient

$$C_L = C_n \cos \alpha - C_c \sin \alpha$$

$$= C_n \text{ in the range of the present tests}$$

C_D — form drag coefficient

$$C_D = C_c \cos \alpha + C_n \sin \alpha$$

$$= C_c + C_L \sin \alpha \text{ in the range of the present tests}$$

C_m — pitching moment coefficient about the local quarter chord point

$$C_m = \int C_p \left(0.25 - \frac{x}{c}\right) d\left(\frac{x}{c}\right)$$

LIST OF REFERENCES

No.	Author	Title, etc.
1	Main-Smith	Chemical solids as diffusible coating films for visual indication of boundary layer transition in air and water. R.& M. 2755 Feb.. 1950
2	Evans	Corrections to velocity for wall constraint in any 10 × 7 subsonic wind tunnel. R. & M. 2662 April, 1949
3	Ackeret, Feldmann and Rott	Investigations on compression shocks and boundary layers in fast moving gases. A.R.C. 10,044 Institute for Aerodynamics E.T.H. Zürich No. 10-1946
4	Rogers, Chinneck and Cash	A comparison of results obtained at high subsonic speeds on two aerofoils having the same section but different chord. A.R.C. 13,628 December 1950
5	Thompson and Adamson	High speed wind tunnel measurements of pressure distribution on an aerofoil of NACA 23021 section. ARC 8350 November 1944
6	Clarke and Gamble	Choking effects and some Reynolds number effects on the Mach number distribution round a two-dimensional aerofoil in the High Speed Tunnel. ARC 13,123 September 1949

Wt.2078.CP.103.K3. Printed in Great Britain.

TABLE 1

Ordinates of Section

R.A.E. 104, 1% camber (NACA camber line $a = 0.6$)

x/c	$100\ y/c$	
	Upper Surface	Lower Surface
0	0	0
0.005	0.9652	0.8770
0.0075	1.1881	1.0647
0.0125	1.5443	1.3557
0.025	2.2007	1.8697
0.05	3.1156	2.5512
0.075	3.7969	3.0357
0.10	4.3464	3.4142
0.15	5.1903	3.9805
0.20	5.8319	4.3815
0.25	6.3025	4.6647
0.30	6.6400	4.8570
0.35	6.8610	4.9710
0.40	6.9752	5.0118
0.45	6.9834	4.9834
0.50	6.8831	4.8831
0.55	6.6632	4.7040
0.60	6.2915	4.4245
0.65	5.7040	4.0012
0.70	4.9866	3.4928
0.75	4.1932	2.9368
0.80	3.3597	2.3569
0.85	2.5129	1.7747
0.90	1.6673	1.1911
0.95	0.8265	0.6027
1.00	0	0

TABLE II

Position of boundary layer transition at pressure plotting section

Upper surface

M	R x 10^{-6}	α^{o}	Position of Transition x/c	Remarks
			Transition free	
0.49	3.5	-0.3	0.67	
0.82	3.5	-0.3	0.67	
"	1.8	"	0.65	
"	0.8	"	0.70	
"	"	"	0.65	Tufts on wing between 50% and 70% chord
			Transition fixed	
0.49	0.8	-0.3	0.20 approx	0.015" dia. thread at x/c = 0.17
0.82	3.5	-0.3	0.08	0.005" " " " x/c = 0.08
"	"	2.7	"	" " " " " Separation from about x/c = 0.53
"	1.8	-0.3	0.60	0.005" dia. thread at x/c = 0.08 Wedges from high spots on thread
"	"	"	0.12	0.010" dia. thread at x/c = 0.12
"	0.8	"	0.58 to 0.62	" " " " " Wedges from high spots on thread
"	"	"	0.20 approx	0.015" dia. thread at x/c = 0.08
"	"	"	0.65 approx	0.015" dia. thread at x/c = 0.37
"	"	"	0.28 approx	16 gauge wire at x/c = -0.57 (i.e. ahead of L.E. of wing)

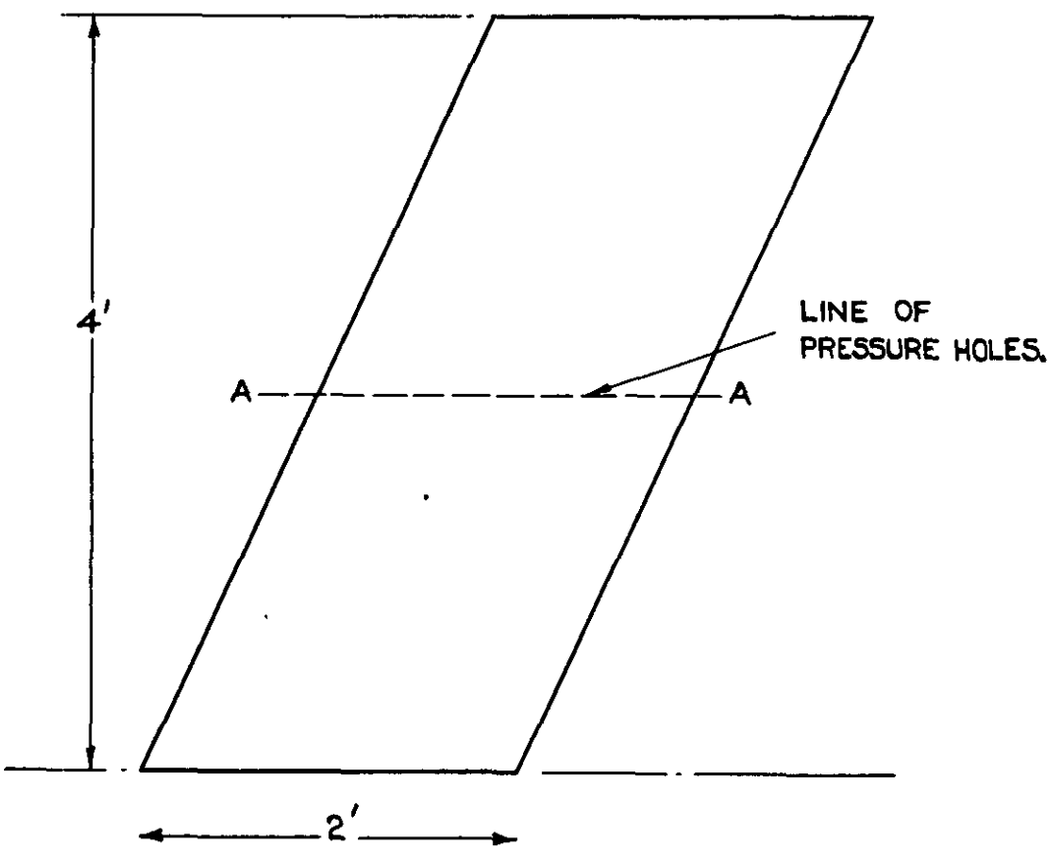

$\phi = 25^\circ$

ASPECT RATIO = 4

SECTION AA - R.A.E 104, 1% CAMBER, $a = 0{\cdot}6$

HALF MODEL

FIG. I. SCALE EFFECT WING.

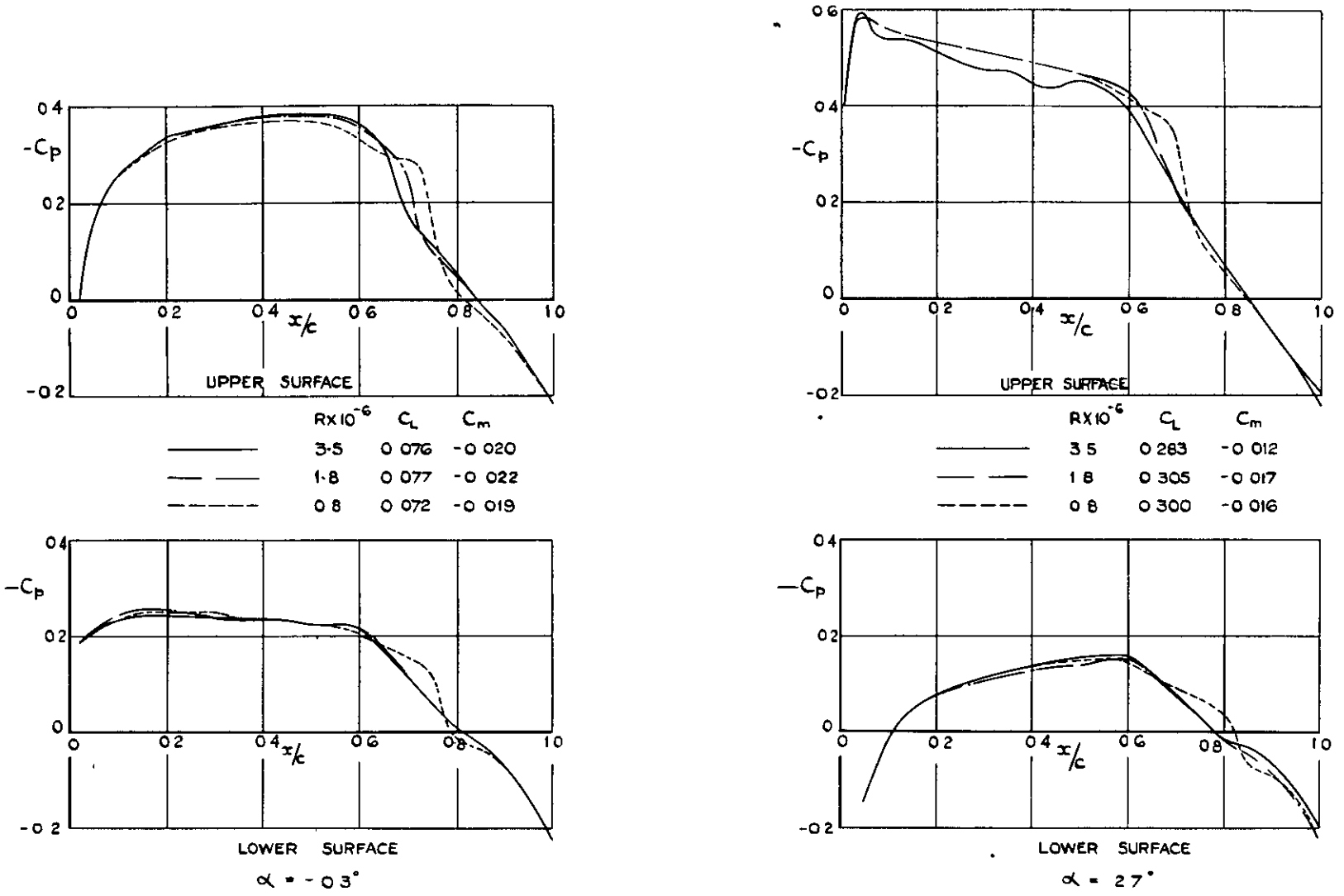

FIG 2. EFFECT OF REYNOLDS NUMBER ON PRESSURE DISTRIBUTIONS AT M = 0·49 TRANSITION FREE.

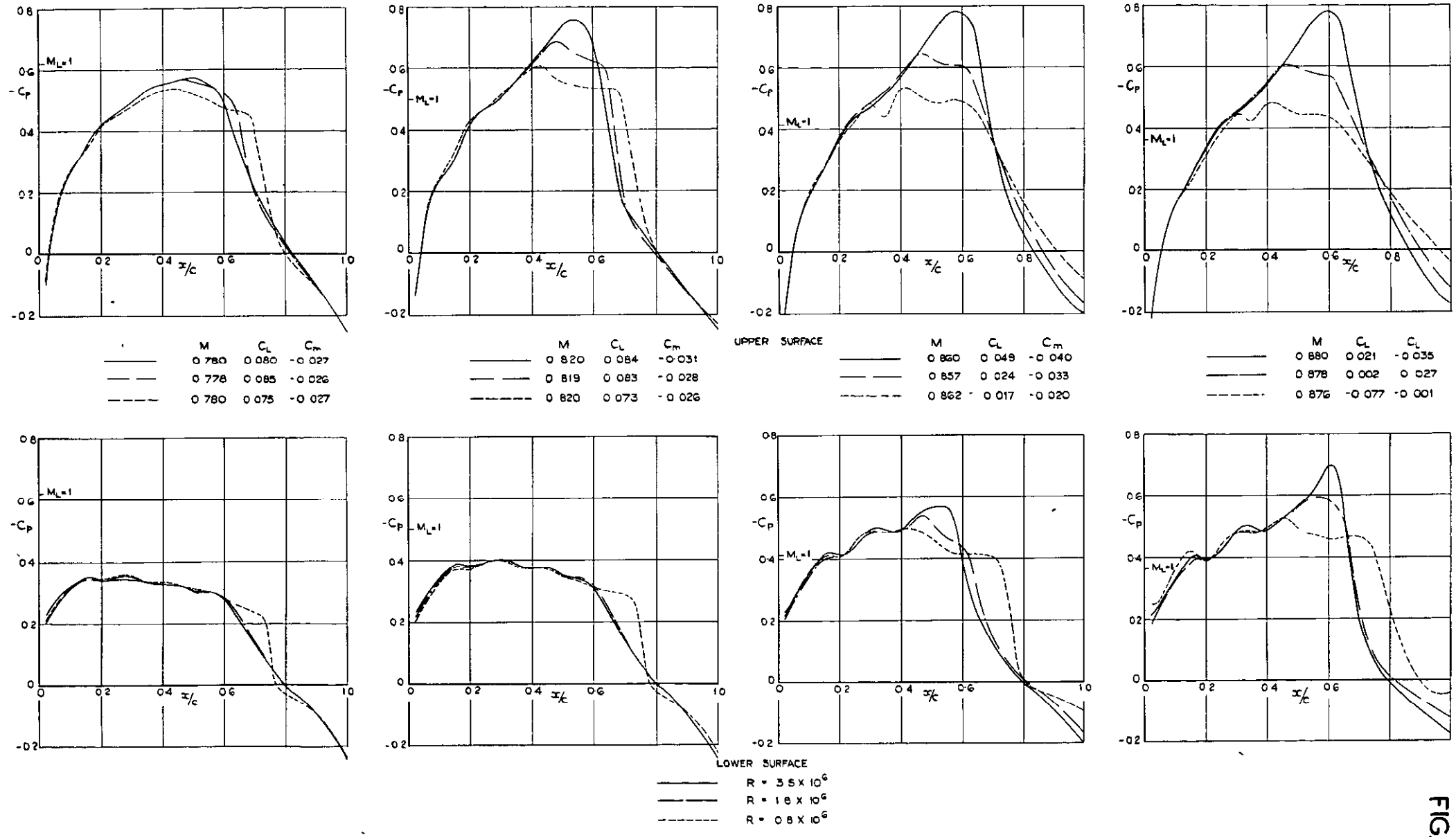

FIG. 3. EFFECT OF REYNOLDS NUMBER ON PRESSURE DISTRIBUTIONS TRANSITION FREE $\alpha \approx -0.3^\circ$.

FIG. 3.

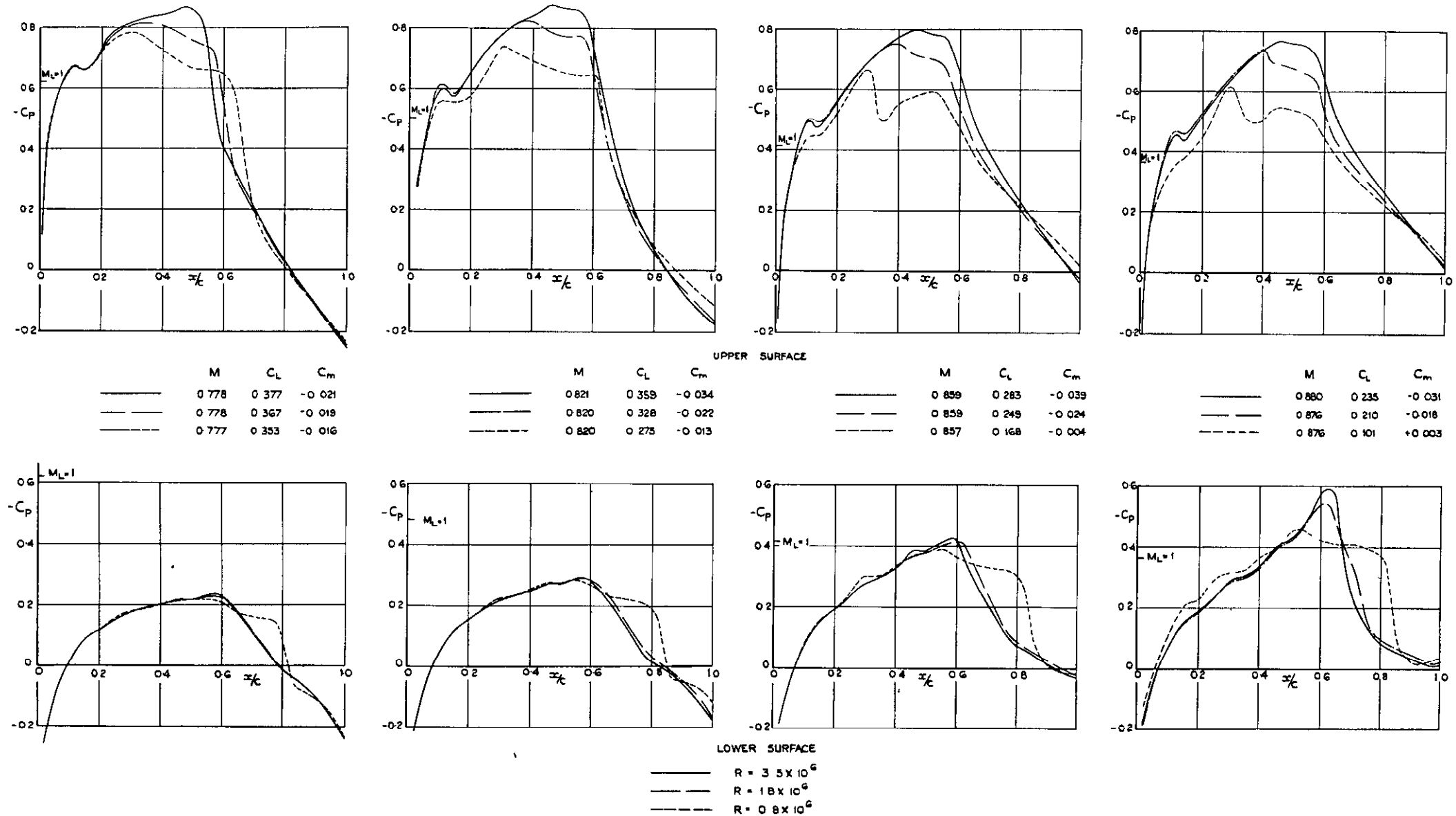

FIG. 4. EFFECT OF REYNOLDS NUMBER ON PRESSURE DISTRIBUTIONS, TRANSITION FREE, $\alpha \approx 2.7°$

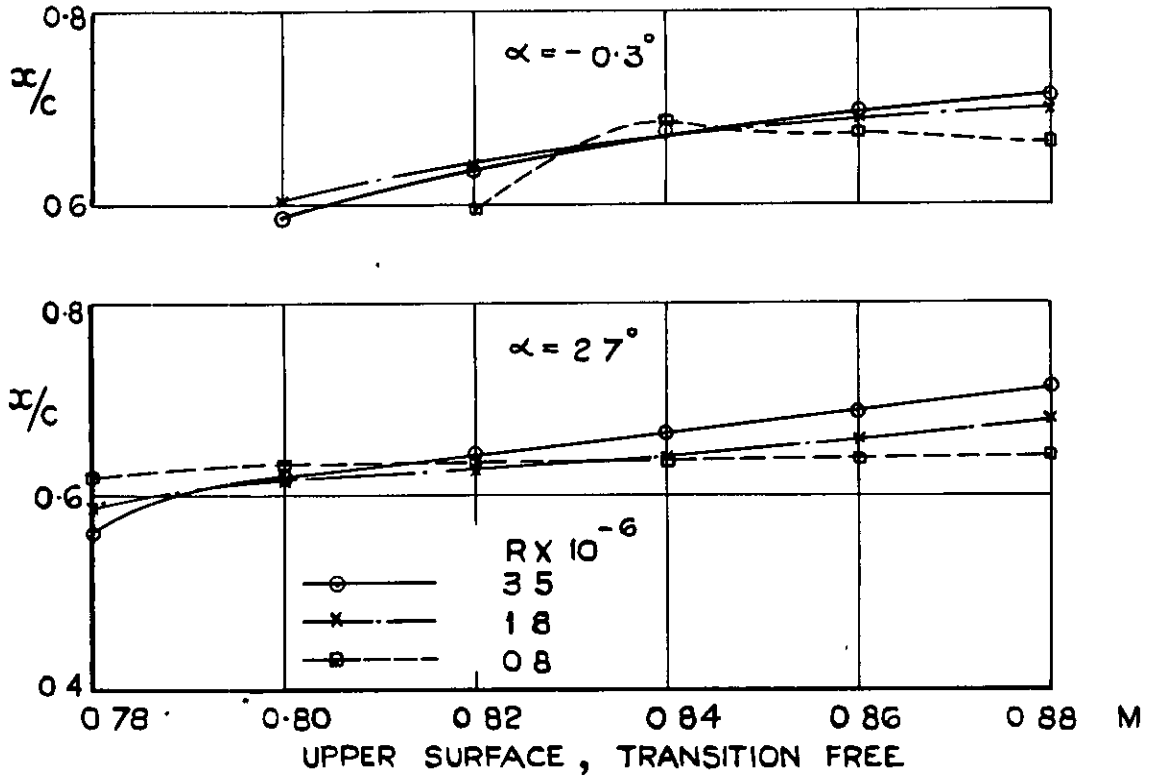

FIG. 5. APPROXIMATE POSITION OF SHOCK WAVE.
(REAR POSITION OF C_p * ALONG AEROFOIL CHORD)

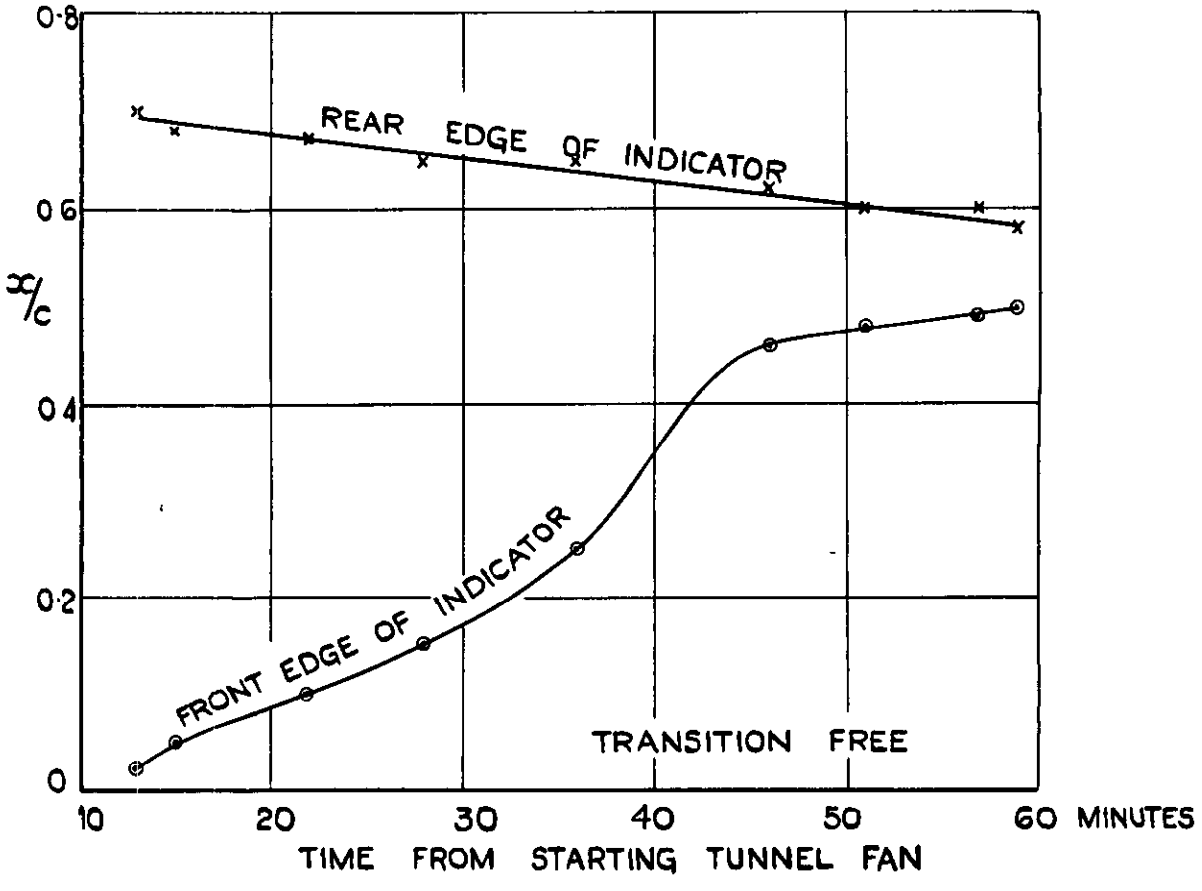

FIG. 6. CHORDWISE EXTENT OF TRANSITION INDICATOR AT M = 0·82, R = 0·8X10⁶, α = 0°.

FIG. 7.

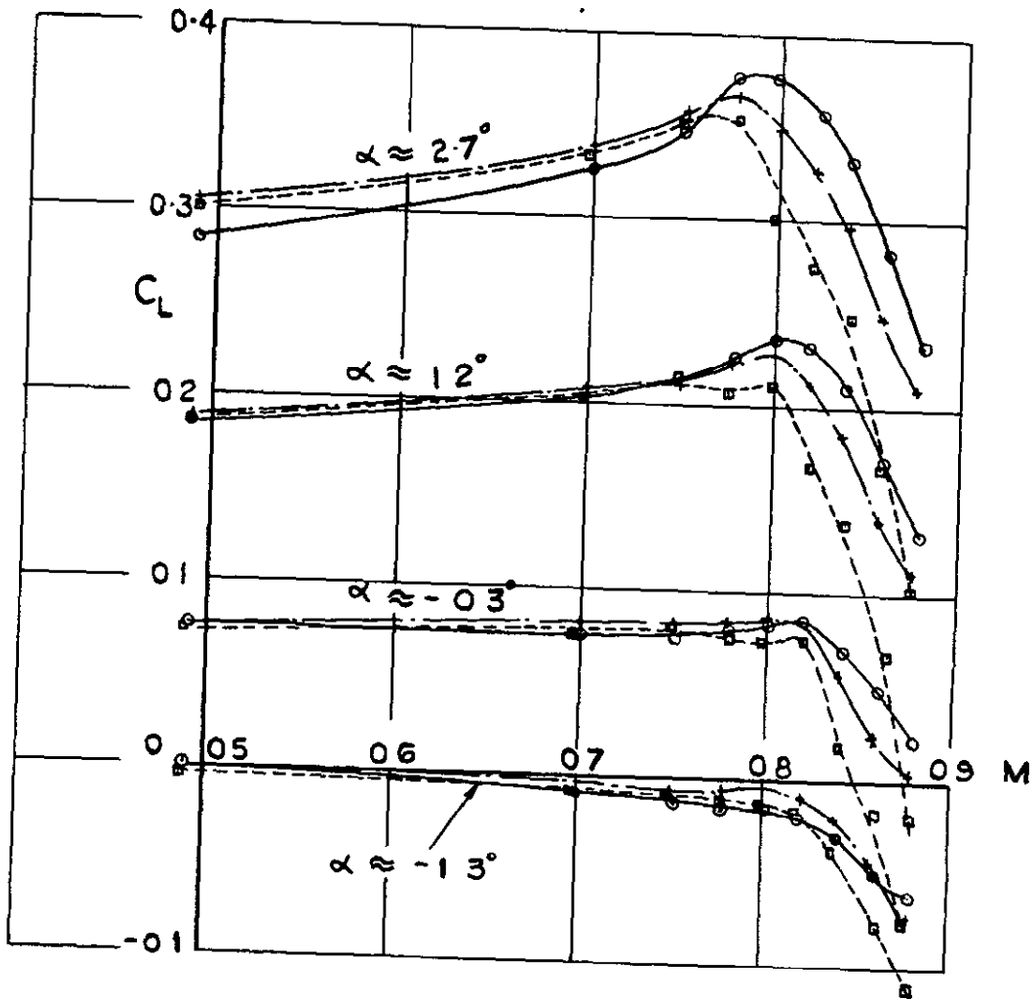

FIG. 7. C_L vs M AT CONST. α.

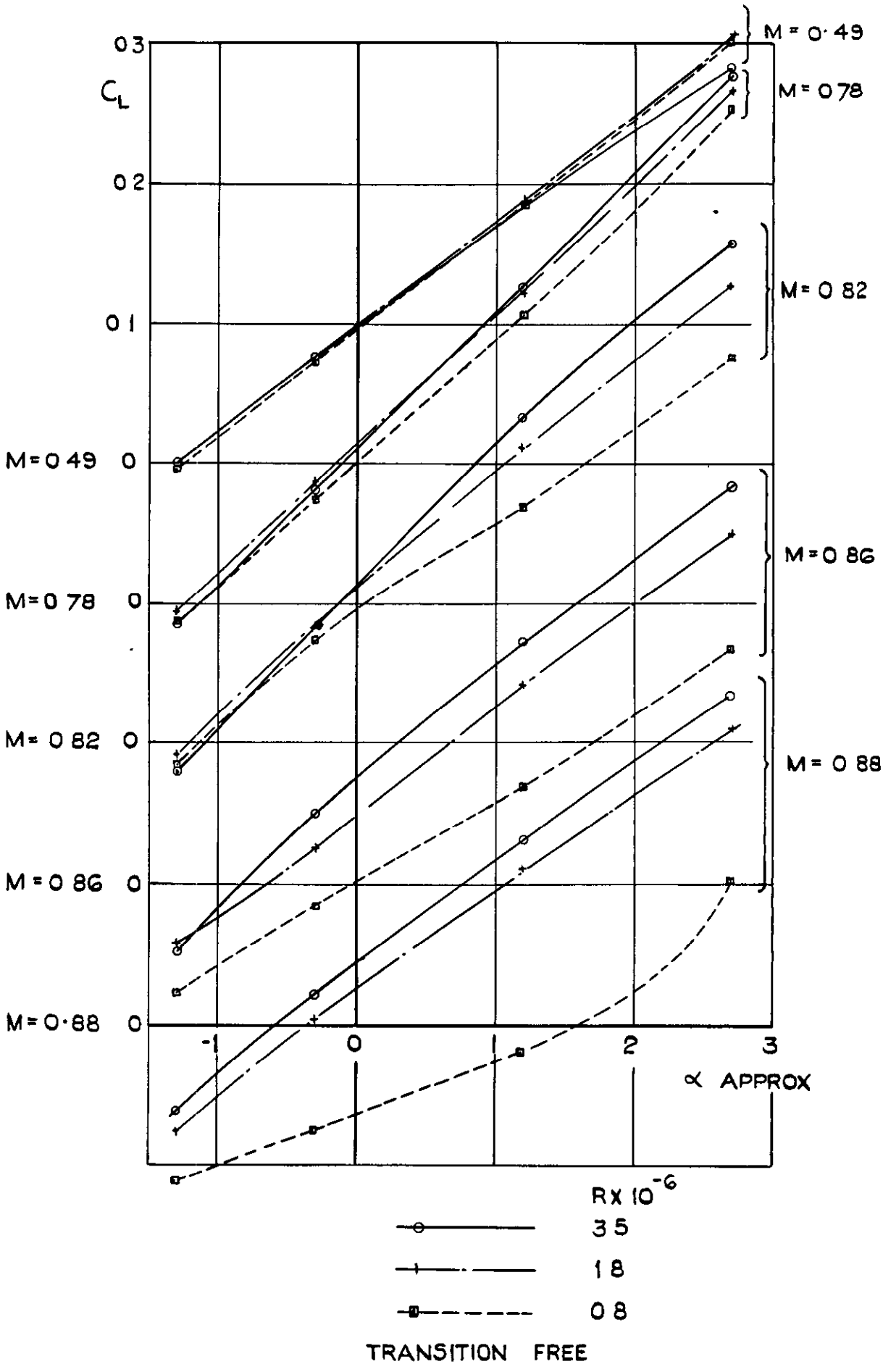

FIG. 8. LIFT CURVES AT CONSTANT MACH NUMBER.

FIG. 9.

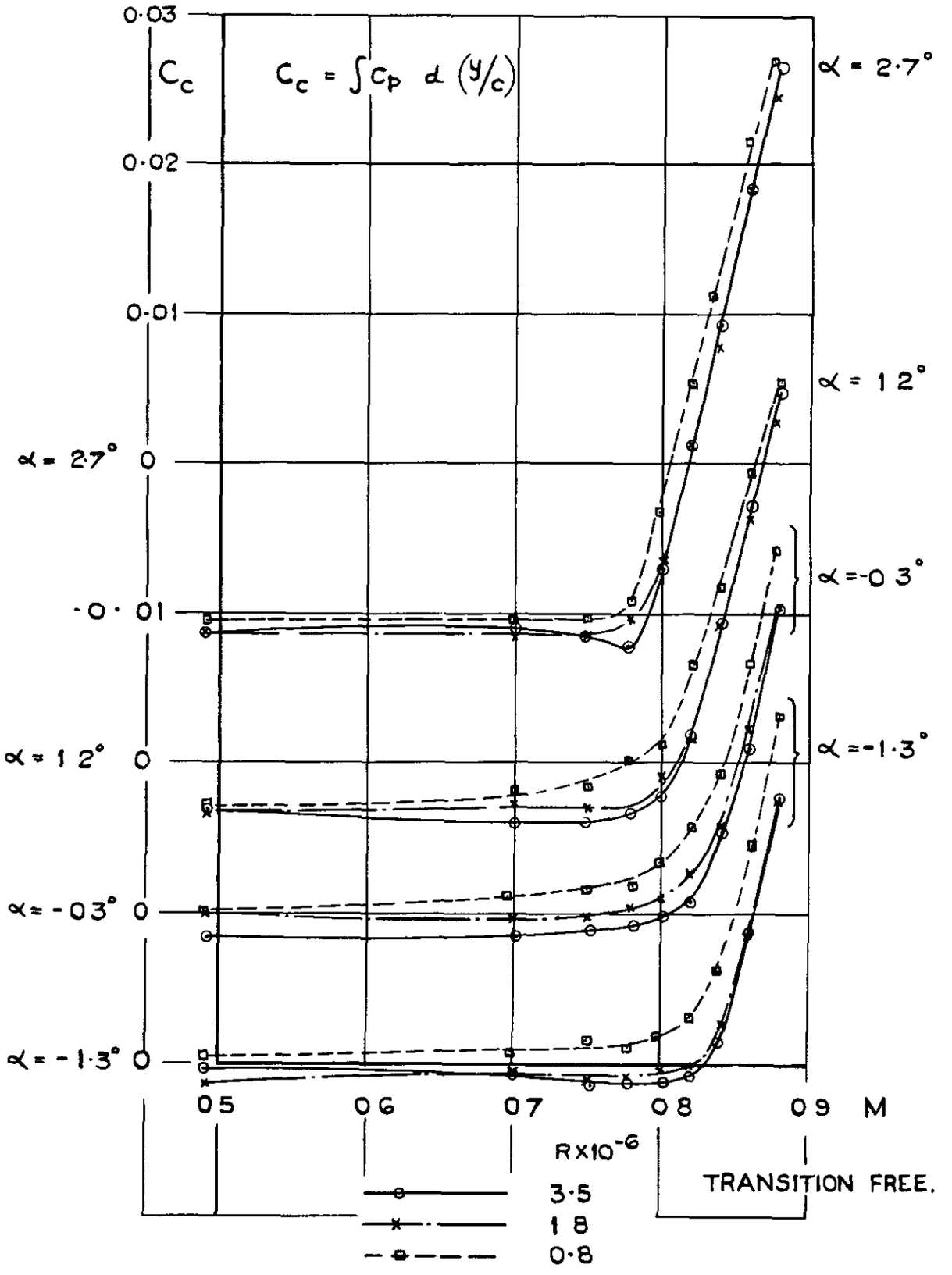

FIG. 9. EFFECT OF REYNOLDS NUMBER ON FORGE COMPONENT ALONG THE CHORD.

FIG. 10

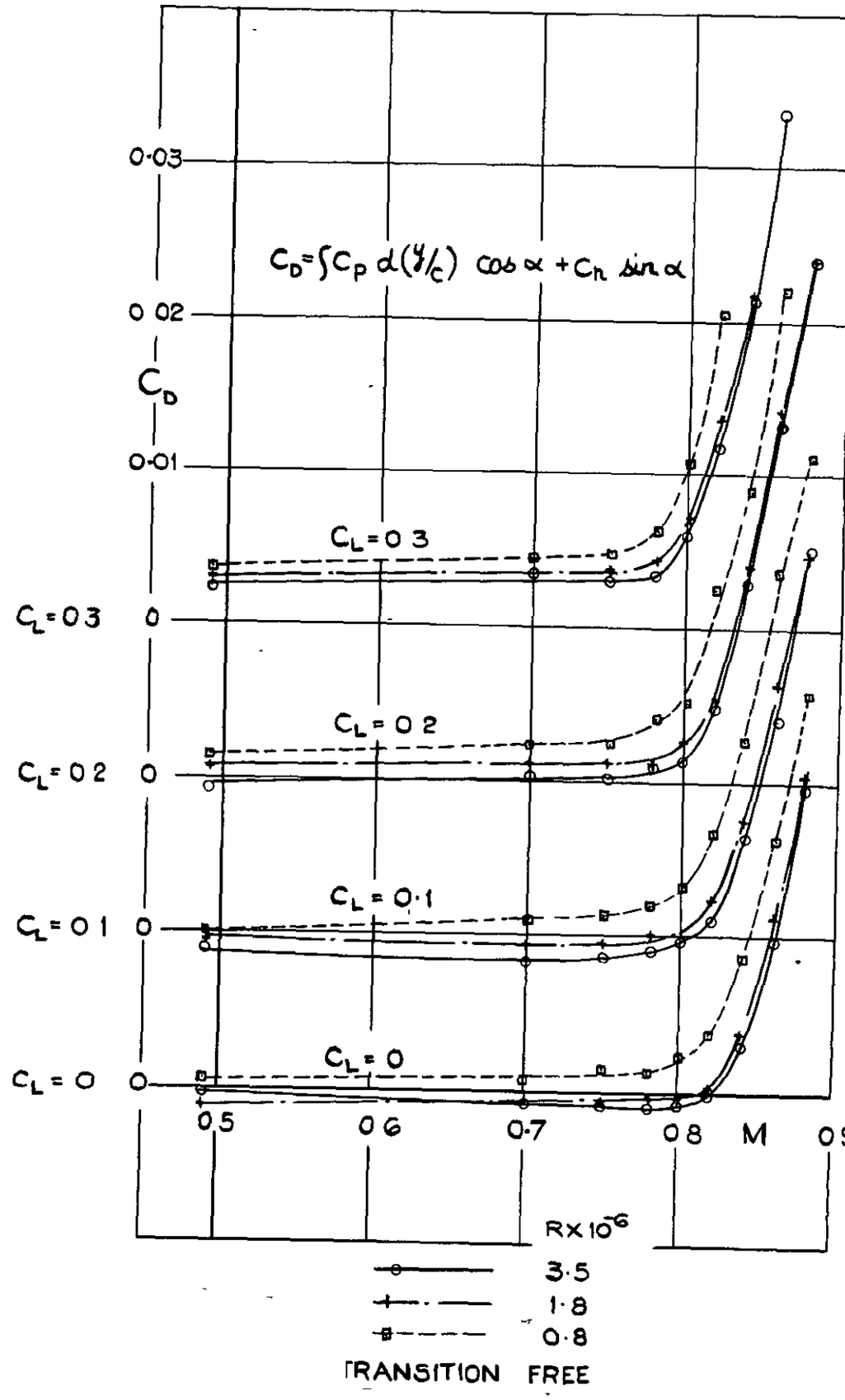

FIG. 10. EFFECT OF REYNOLDS NUMBER ON FORM DRAG.

FIG. 11.

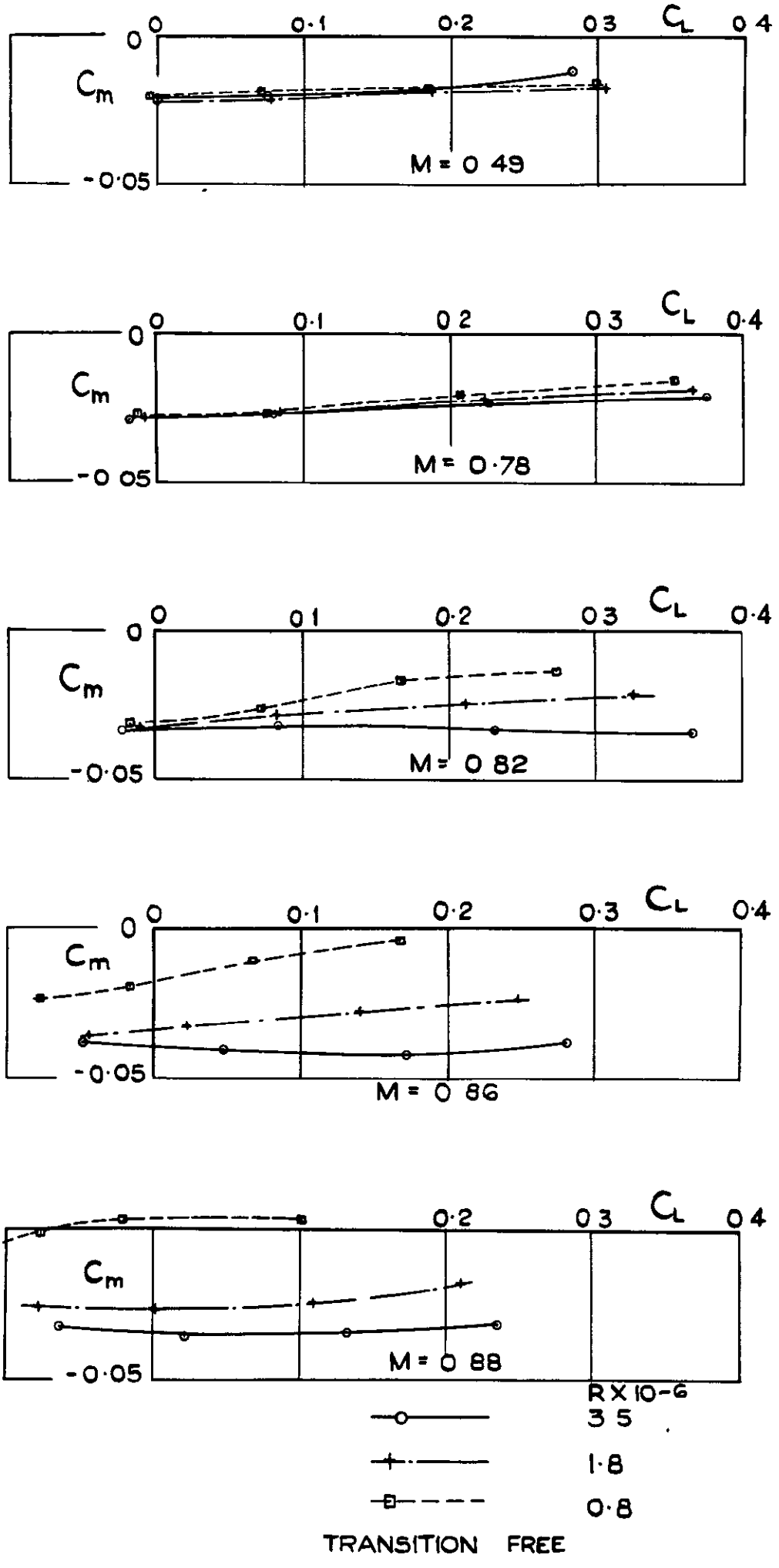

FIG. 11. C_m vs C_L CURVES AT CONSTANT MACH NUMBER.

FIG. 12.

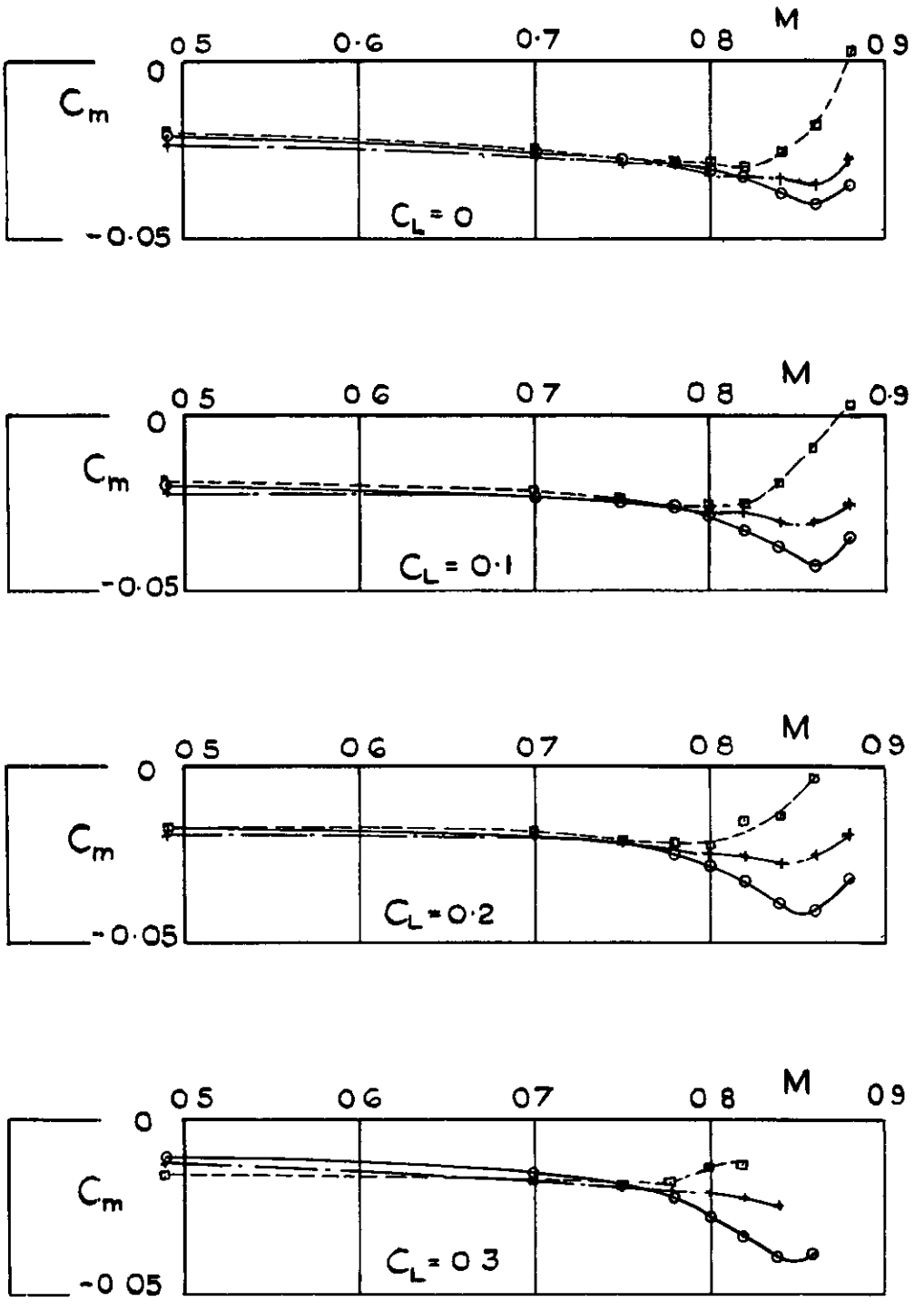

FIG. 12. C_m vs M AT CONSTANT C_L.

FIG.13 & 14.

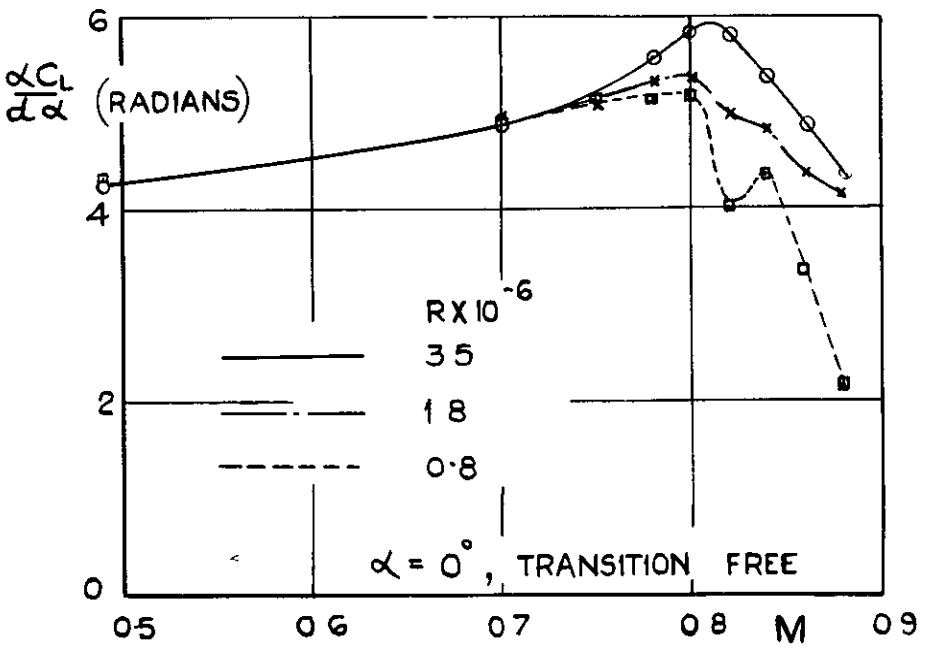

FIG. 13. EFFECT OF REYNOLDS NUMBER ON LIFT CURVE SLOPE.

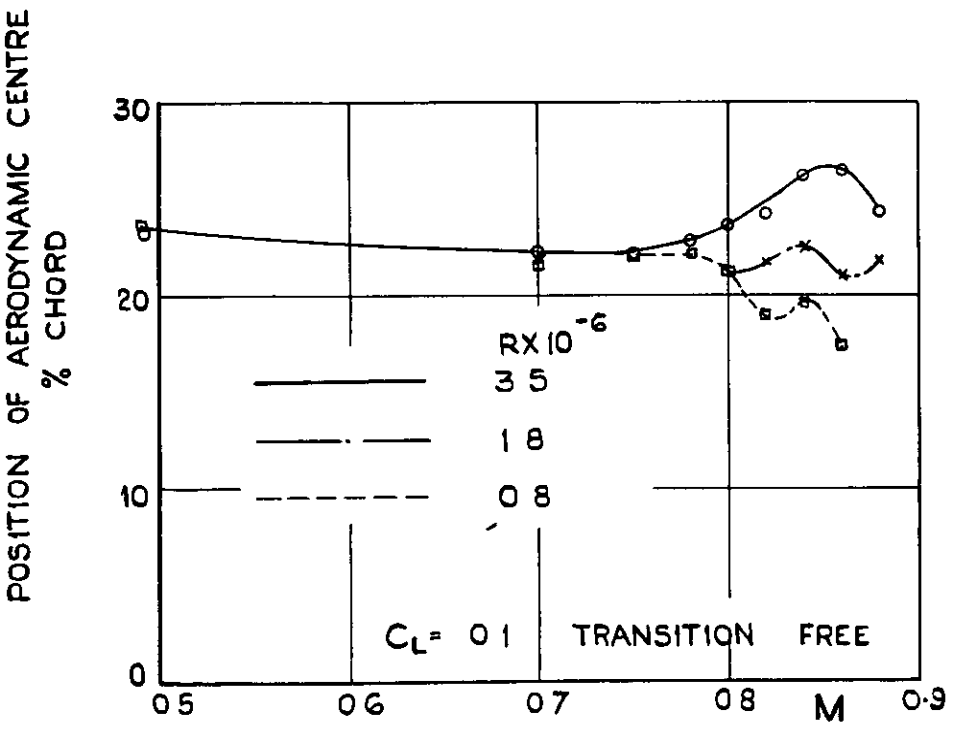

FIG. 14. EFFECT OF REYNOLDS NUMBER ON POSITION OF AERODYNAMIC CENTRE.

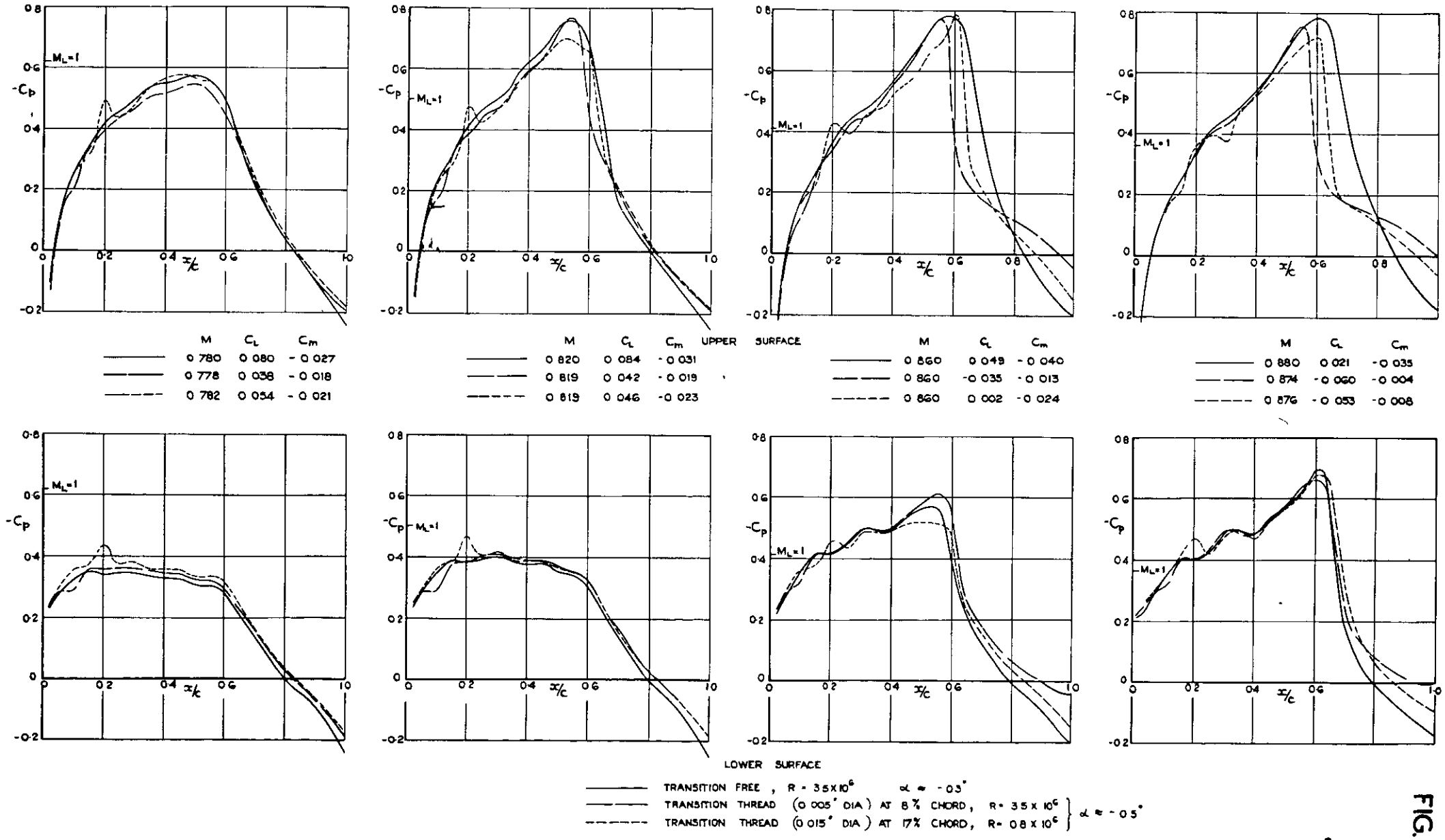

FIG. 15. EFFECT OF TRANSITION THREADS ON BOTH SURFACES OF WING, $\alpha \approx -0.3^{\circ}$.

FIG. 15.

FIG.16.

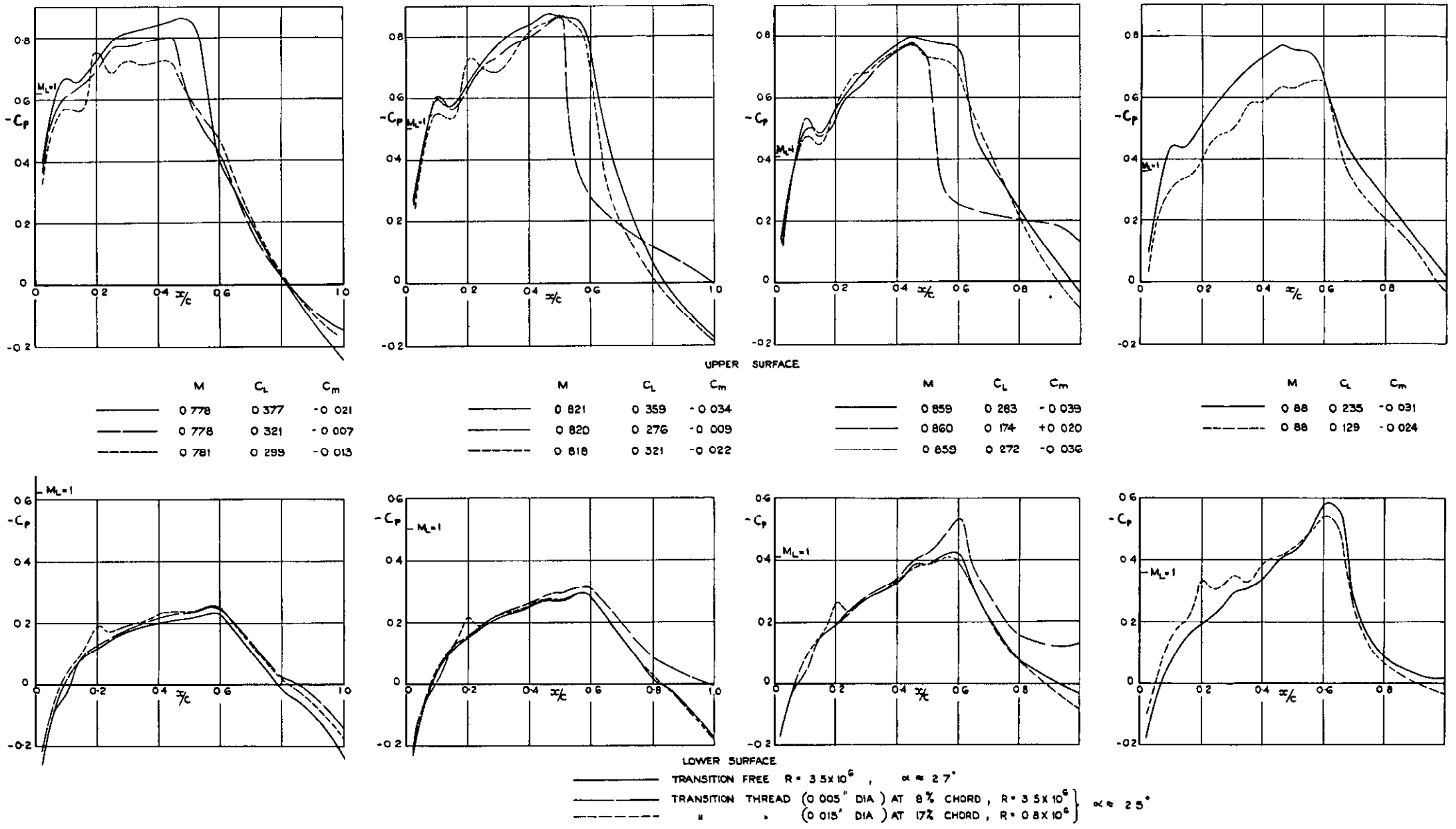

FIG. 16. EFFECT OF TRANSITION THREADS ON BOTH SURFACES OF WING, $\alpha \approx 2{\cdot}7°$.

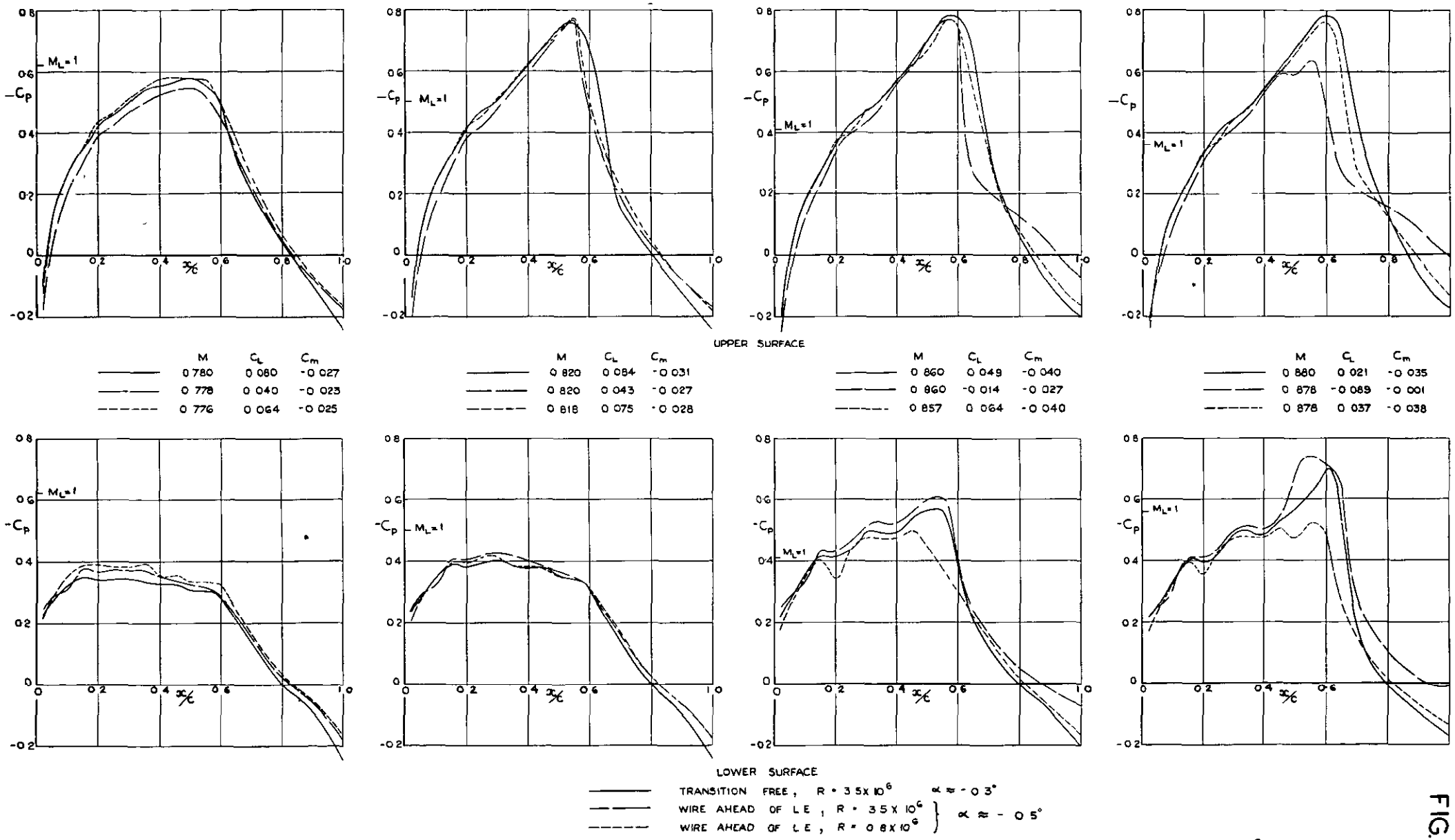

FIG 17 EFFECT OF WIRE O 57c AHEAD OF WING LEADING EDGE, $\alpha \approx 0\,3^\circ$.

FIG.17

FIG. 18(a & b)

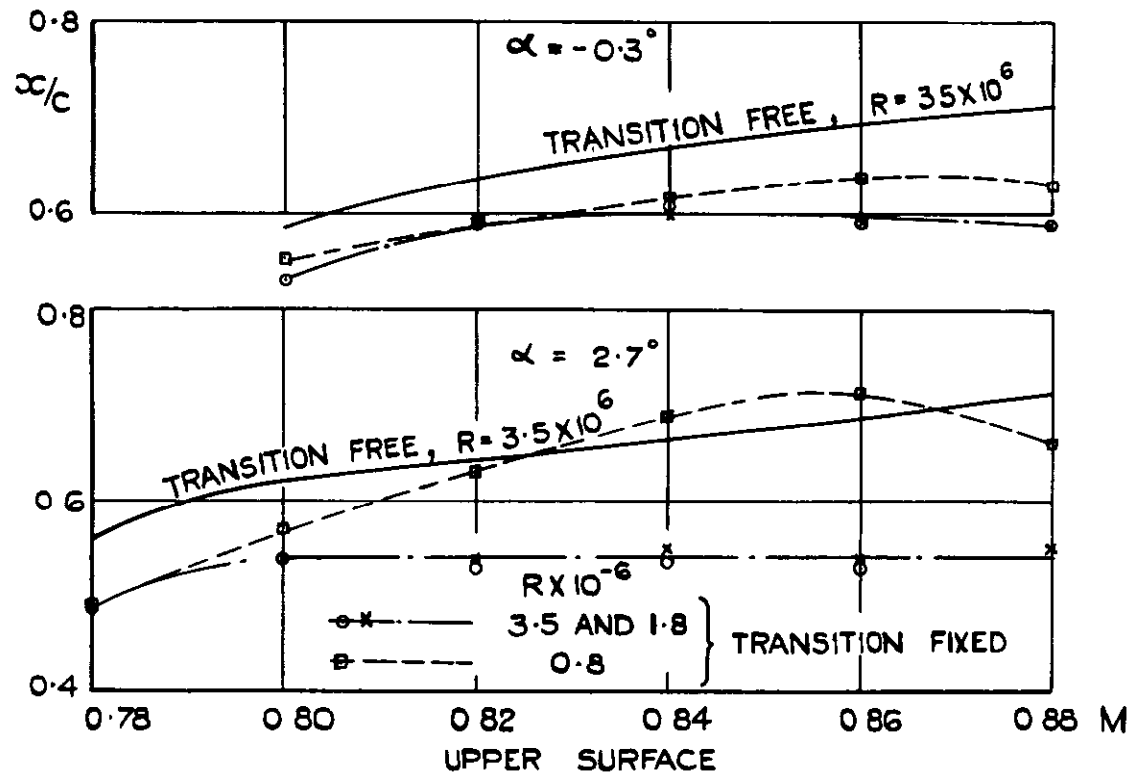

FIG. 18 (a) APPROXIMATE POSITION OF SHOCKWAVE.

(REAR POSITION OF C_p* ALONG AEROFOIL CHORD)

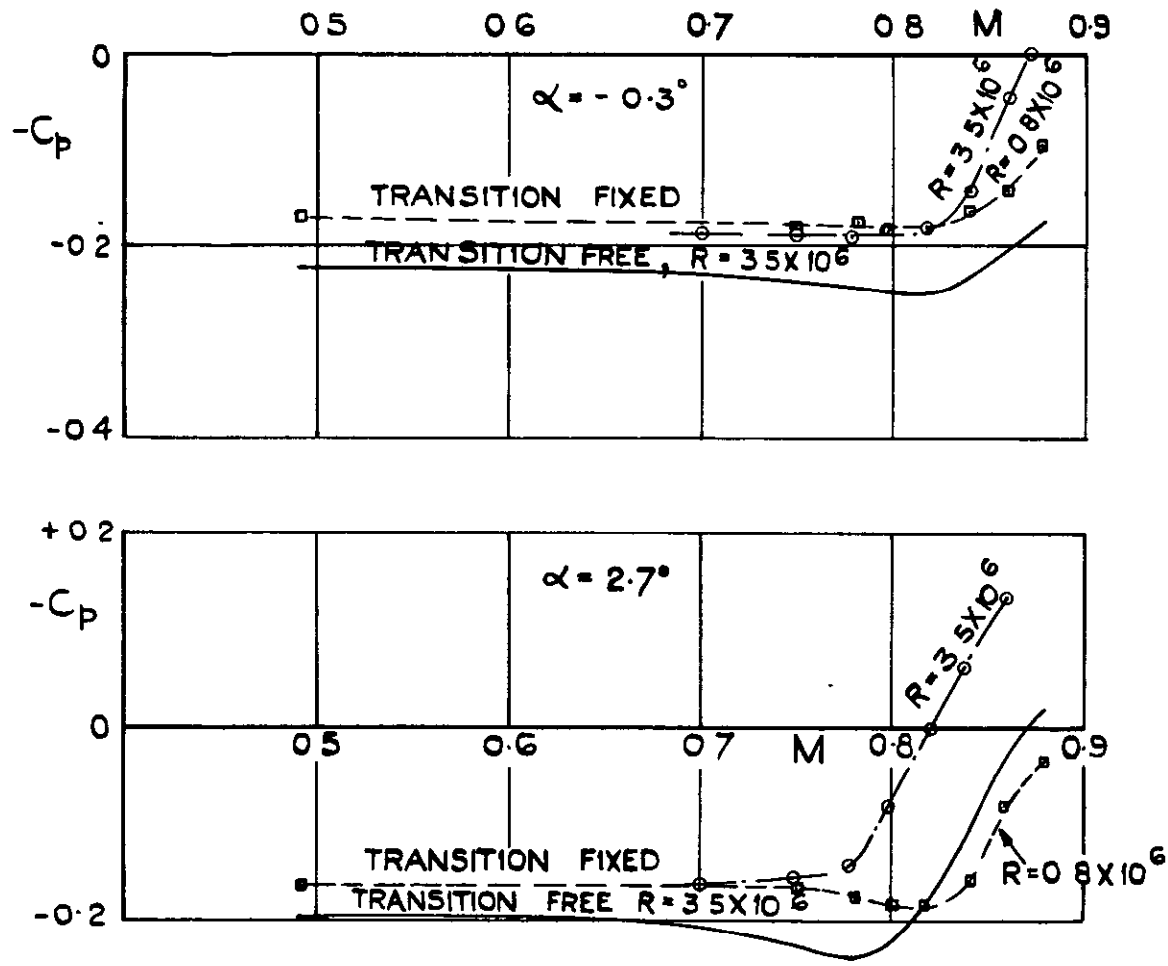

FIG. 18 (b) TRAILING EDGE SUCTIONS. EFFECT OF FIXING TRANSITION BY THREADS ON SHOCKWAVE POSITION & T.E. SUCTIONS.

FIG. 19.

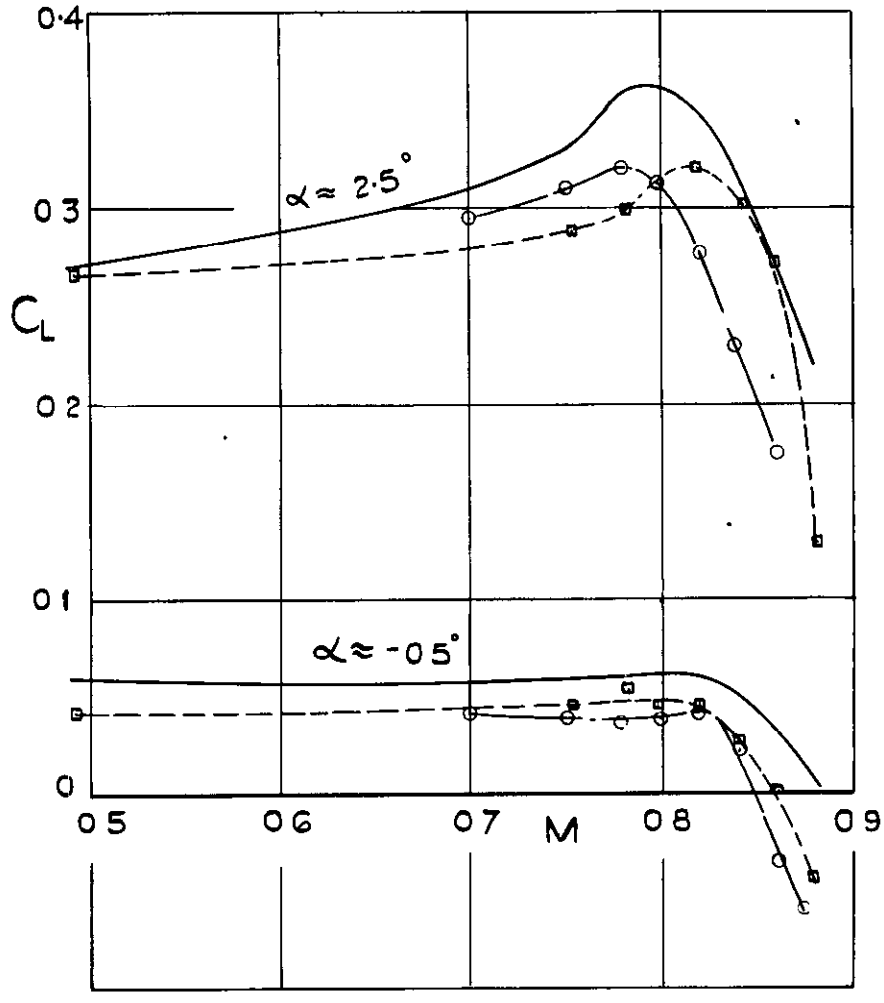

——— TRANSITION FREE, $R = 3.5 \times 10^6$

—o— 0 005" DIA THREAD AT 8% CHORD, $R \approx 3.5 \times 10^6$

– –□– – – 0 015" DIA THREAD AT 17% CHORD, $R \approx 0.8 \times 10^6$

TRANSITION FIXED BY THREADS ON BOTH WING SURFACES.

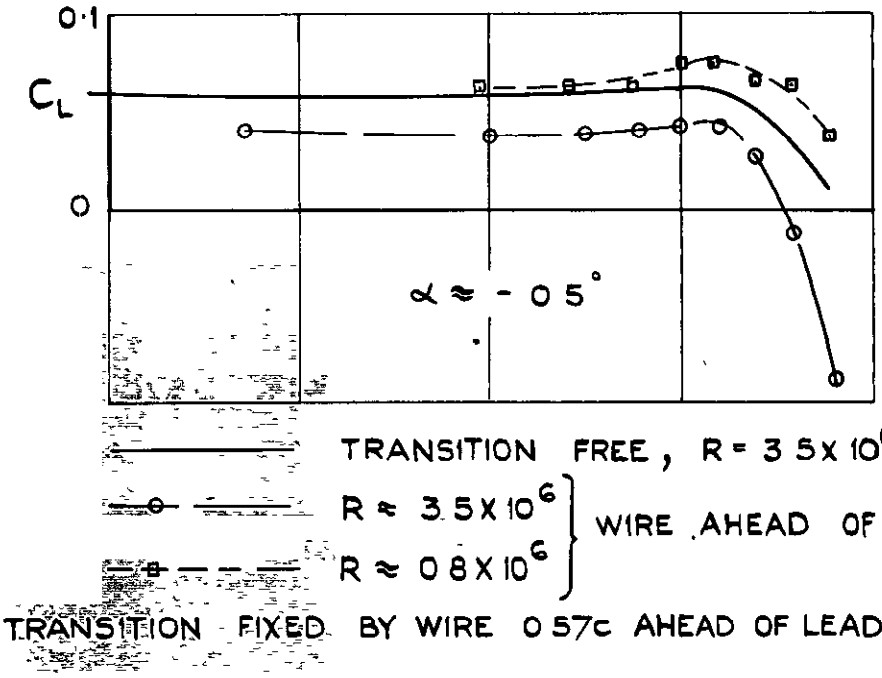

——— TRANSITION FREE, $R = 3.5 \times 10^6$

—o— $R \approx 3.5 \times 10^6$ } WIRE AHEAD OF L.E.

– –□– – $R \approx 0.8 \times 10^6$ }

TRANSITION FIXED BY WIRE 0·57c AHEAD OF LEADING EDGE

FIG. 19. EFFECT ON C_L OF FIXING TRANSITION.

FIG. 20.

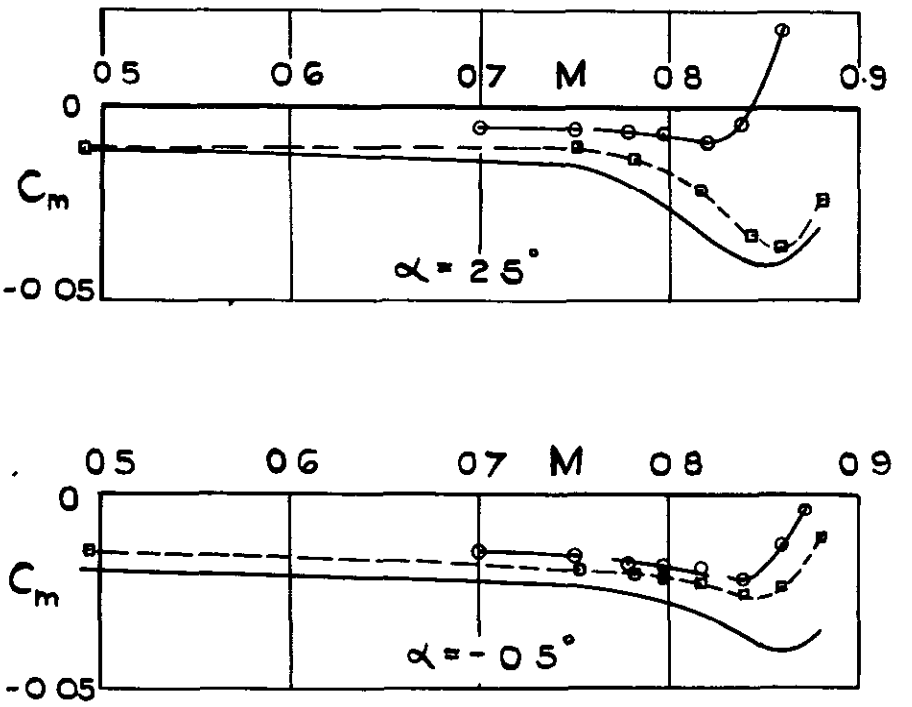

——— TRANSITION FREE, $R = 3.5 \times 10^6$

—o— 0·005" DIA. THREAD AT 8% CHORD, $R = 3.5 \times 10^6$

—▪— 0·015" DIA. THREAD AT 17% CHORD, $R = 0.8 \times 10^6$

TRANSITION FIXED BY THREADS ON BOTH WING SURFACES.

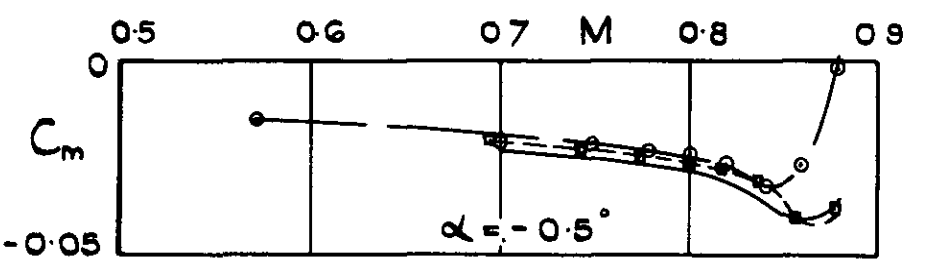

——— TRANSITION FREE, $R = 3.5 \times 10^6$

—o— $R = 3.5 \times 10^6$ } WIRE AHEAD OF L.E.

—▪— $R = 0.8 \times 10^6$ }

TRANSITION FIXED BY WIRE 0·57c AHEAD OF L.E.

FIG. 20. EFFECT ON C_m OF FIXING TRANSITION.

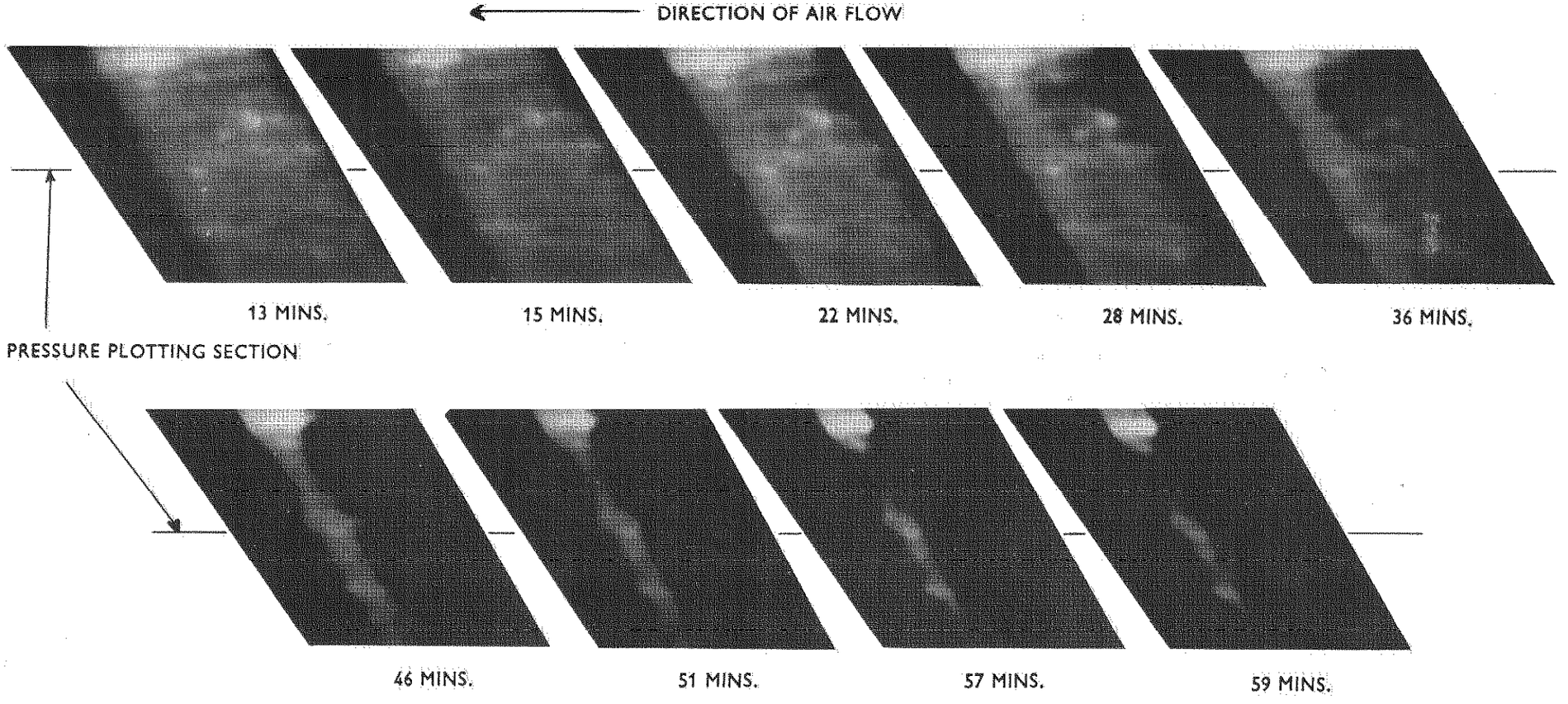

$M = 0{\cdot}82$, $R = 0{\cdot}8 \times 10^6$, $\alpha = 0{\cdot}3°$, TRANSITION FREE

FIG.21. TRANSITION INDICATOR ON SCALE EFFECT WING

(ONLY PART OF THE WING IS SHOWN)

FIG.21

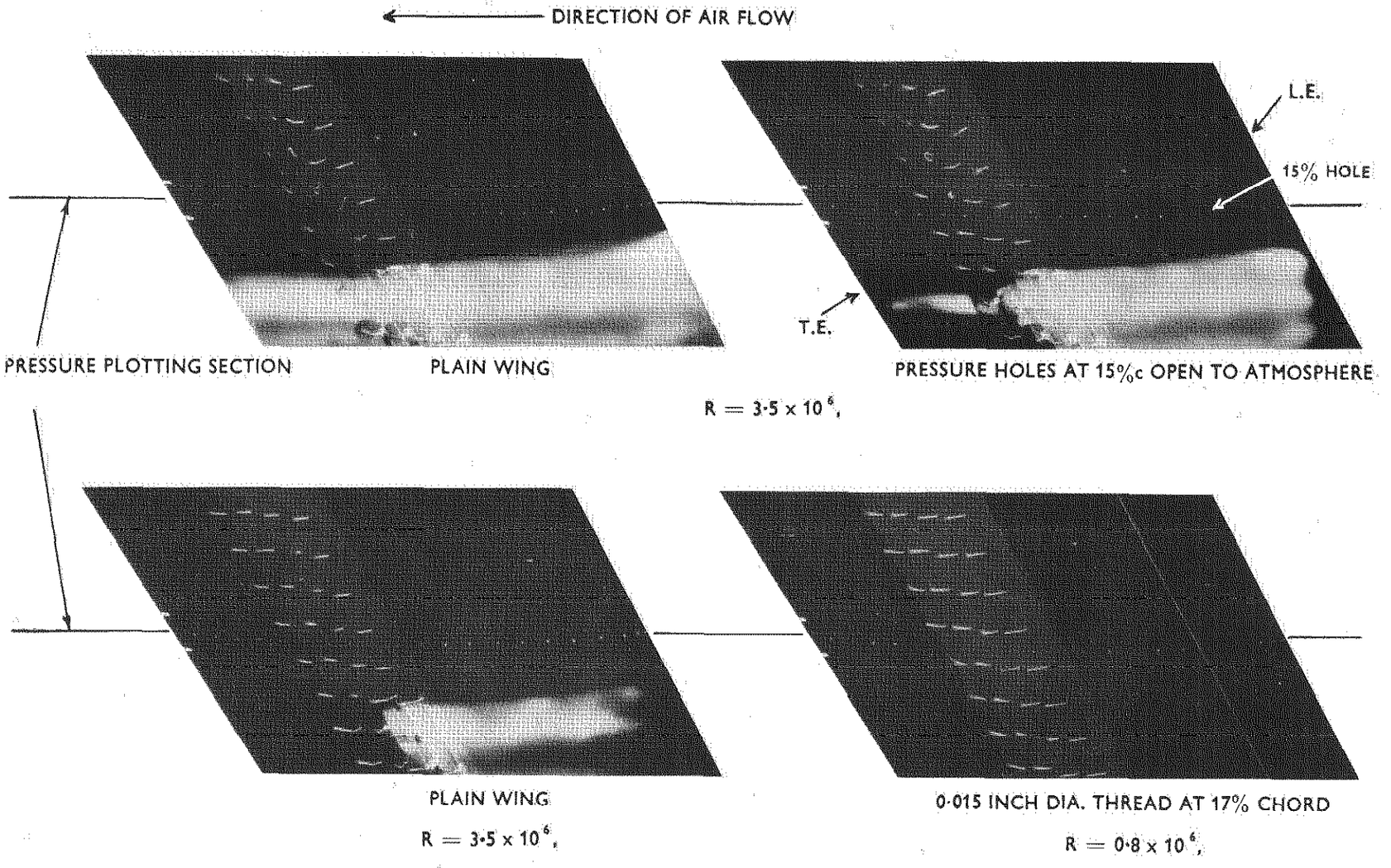

FIG.22. TUFTS ON SCALE EFFECT WING AT M = 0·82, α = -0·3°

(ONLY PART OF THE WING IS SHOWN)

FIG.22

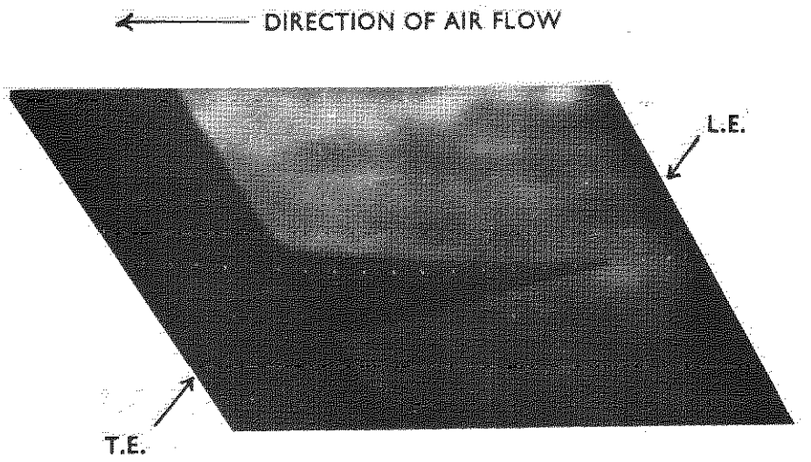

$R = 3{\cdot}5 \times 10^6$, $M = 0{\cdot}49$

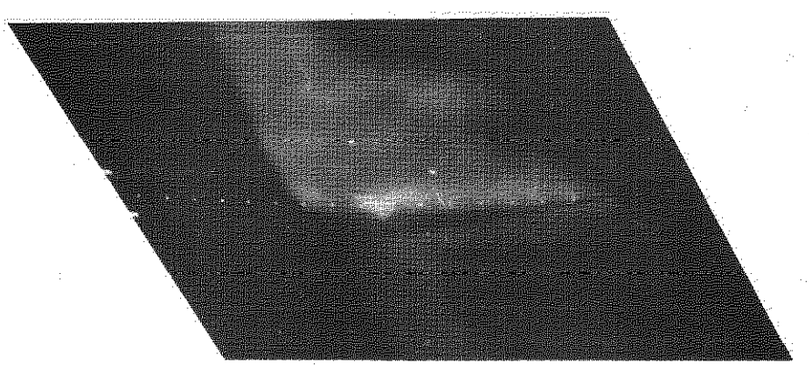

$R = 0{\cdot}8 \times 10^6$, $M = 0{\cdot}82$.

FIG.23. TRANSITION WEDGES CAUSED BY JET OF AIR ISSUING FROM 15%c PRESSURE HOLE

C.P. No. 103
(14,448)
A.R.C. Technical Report

PUBLISHED BY HER MAJESTY'S STATIONERY OFFICE

To be purchased from

York House, Kingsway, LONDON, W.C.2: 429 Oxford Street, LONDON, W.1
P.O. Box 569, LONDON, S.E.1
13a Castle Street, EDINBURGH, 2 | 1 St. Andrew's Crescent, CARDIFF
39 King Street, MANCHESTER, 2 | Tower Lane, BRISTOL, 1
2 Edmund Street, BIRMINGHAM, 3 | 80 Chichester Street, BELFAST
or from any Bookseller

PRINTED IN GREAT BRITAIN

1952

Price 5s. 0d. net

S.O. Code No. 23-9007-3